

LEVEL II (2)

FRANK J. SEILER RESEARCH LABORATORY

FJSRL-TR-81-0007

JULY 1981



A TWO-DEGREE-OF-FREEDOM
OSCILLATOR FOR
UNSTEADY AERODYNAMICS APPLICATIONS

PRELIMINARY REPORT

DTIC
ELECTE
AUG 03 1981
S E D

CAPT M.S. FRANCIS
CAPT J.E. KEESEE
MAJ J.P. RETELLE, JR.

APPROVED FOR PUBLIC RELEASE;
DISTRIBUTION UNLIMITED.

PROJECT 2307

AIR FORCE SYSTEMS COMMAND
UNITED STATES AIR FORCE

81 7 31 066

AD A102356



FILE COPY

FJSRL-TR-81-0007

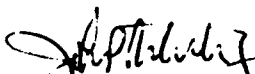
This document was prepared by the Mechanics Division, Directorate of Aerospace-Mechanics Sciences, Frank J. Seiler Research Laboratory, United States Air Force Academy, Colorado. The research was conducted under Project Work Unit Number 2307-F1-36, An Investigation of Unsteady Vortex Entrapment on an Airfoil. Major John P. Retelle, Jr. was the Principal Investigator in charge of the work.

When U.S. Government drawings, specifications or other data are used for any purpose other than a definitely related Government procurement operation, the Government thereby incurs no responsibility nor any obligation whatsoever, and the fact that the Government may have formulated, furnished or in any way supplied the said drawings, specifications or other data is not to be regarded by implication or otherwise, as in any manner licensing the holder or any other person or corporation or conveying any rights or permission to manufacture, use or sell any patented invention that may in any way be related thereto.


Inquiries concerning the technical content of this document should be addressed to the Frank J. Seiler Research Laboratory (AFSC), FJSRL/NH, USAF Academy, Colorado 80840. Phone AC 303-472-3122.

This report has been reviewed by the Commander and is releasable to the National Technical Information Service (NTIS). At NTIS it will be available to the general public, including foreign nations.

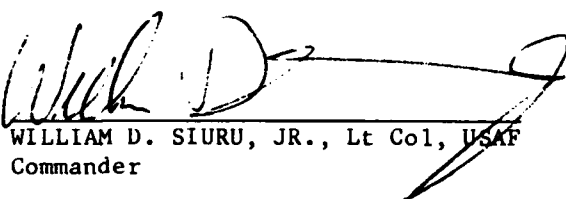
This technical report has been reviewed and is approved for publication.



JOHN P. RETELLE, JR., Major, USAF
Principal Investigator



THEODORE T. SAITO, Lt. Col, USAF
Director
Aerospace-Mechanics Sciences



WILLIAM D. SIURU, JR., Lt Col, USAF
Commander

Copies of this report should not be returned unless return is required by security considerations, contractual obligations, or notice on a specific document.

Printed in the United States of America. Qualified requestors may obtain additional copies from the Defense Documentation Center. All others should apply to: National Technical Information Service
5285 Port Royal Road
Springfield, Virginia 22161

UNCLASSIFIED

SECURITY CLASSIFICATION OF THIS PAGE (When Data Entered)

14 REPORT DOCUMENTATION PAGE		READ INSTRUCTIONS BEFORE COMPLETING FORM
1. REPORT NUMBER FJSRL-TR-81-0007 ADA	2. GOVT ACCESSION NO. AD-A10235	3. RECIPIENT'S CATALOG NUMBER 6 (9)
4. TITLE (and Subtitle) A Two-degree-of-freedom Oscillator for Unsteady Aerodynamics Applications.	5. TYPE OF REPORT & PERIOD COVERED Preliminary rept. Oct 78 - Jul 81	
7. AUTHOR Captain M.S. Francis Captain J.E. Keesee Major J.P. Retelle, Jr.	6. PERFORMING ORG. REPORT NUMBER	
9. PERFORMING ORGANIZATION NAME AND ADDRESS Frank J. Seiler Research Laboratory (AFSC) USAF Academy, CO 80840	8. CONTRACT OR GRANT NUMBER(s)	
11. CONTROLLING OFFICE NAME AND ADDRESS Frank J. Seiler Research Laboratory (AFSC) USAF Academy, CO 80840	10. PROGRAM ELEMENT, PROJECT, TASK AREA & WORK UNIT NUMBERS DRS 61102F 2367-FL-36	
14. MONITORING AGENCY NAME & ADDRESS (if different from Controlling Office) 12/63	12. REPORT DATE July 1981	
	13. NUMBER OF PAGES 62	
	15. SECURITY CLASS. (of this report) UNCLASSIFIED	
16. DISTRIBUTION STATEMENT (of this Report) Approved for public release; distribution unlimited.	15a. DECLASSIFICATION/DOWNGRADING SCHEDULE	
17. DISTRIBUTION STATEMENT (of the abstract entered in Block 20, if different from Report)		
18. SUPPLEMENTARY NOTES		
19. KEY WORDS (Continue on reverse side if necessary and identify by block number) Unsteady flow Oscillating flow Dynamic stall Wind tunnel Computer control		
20. ABSTRACT (Continue on reverse side if necessary and identify by block number) Numerous wind tunnel studies of airfoil dynamic stall have been limited to harmonic model oscillations, but new microcomputers and hybrid servo systems have now been exploited to produce a mechanism which provides a high degree of flexibility in achieving arbitrary model motions in multiple degrees of freedom over a wide range of motion alternatives. A prototype apparatus has been fabricated to provide simultaneous motions of an airfoil or wing model in both pitch and translation. Drive motors provide independent motion in two axes		

DD FORM 1473 1 JAN 73 EDITION OF 1 NOV 65 IS OBSOLETE

UNCLASSIFIED 319920
SECURITY CLASSIFICATION OF THIS PAGE (When Data Entered)

Next page

Item 20 continued.

under the control of servo-translator units which respond to pulse trains generated by the microcomputer, using analog position and feedback loops to smooth the pulses. Programs are developed in a higher-level language using a larger disk-based computer system and then the program task image is downline-loaded through a network communications link to the smaller computer. In addition to a thorough description of the experimental apparatus, the various elements of motion control, including servo-translator dynamic characteristics, software techniques for pulse train generation, and required computer interface circuitry are discussed. Measurements of constant rate, constant acceleration, and pure harmonic motions are examined for both drive axes over the entire range of drive parameters.

TABLE OF CONTENTS

<u>CHAPTER</u>	<u>PAGE</u>
I. INTRODUCTION	1
II. MECHANICAL DESIGN	3
A. MOTION TRANSFER APPARATUS	3
B. PITCH DRIVE ASSEMBLY	3
C. MODEL AND MODEL INTERFACE	6
D. TRANSLATIONAL DRIVE ASSEMBLY	7
E. FACILITY INTERFACE	8
III. SERVO-DRIVE ELECTRONICS	10
IV. COMPUTER COMMAND SYSTEM	14
A. PULSE TRAIN REQUIREMENTS	14
B. HARDWARE	15
C. SOFTWARE	17
V. PERFORMANCE	20
VI. SUMMARY	25
REFERENCES	26
ACKNOWLEDGEMENTS	27
FIGURES	28

Accession For	
NTIS GRA&I	<input checked="" type="checkbox"/>
DTIC TAB	<input type="checkbox"/>
Unannounced	<input type="checkbox"/>
Justification	
By _____	
Distribution/ _____	
Availability Codes	
Dist	Avail and/or Special
A	

LIST OF FIGURES

<u>#</u>	<u>TITLE</u>
1	Two-Degree-of-Freedom Apparatus, Functional Schematic
2	Mechanical Oscillation Assembly
3	Pitch Yoke Sub-Assembly
4	SM708 Series Motor - Description
5	Model Mounting Detail
6	NACA 0012 Airfoil Model and Instrumentation
7	Translational Drive Assembly
8	Experiment Installed in USAFA 2 ft x 3 ft Subsonic Wind Tunnel
9	Neoprene Slot Seal
10	Servo Drive Electronics - Schematic
11	Servo Translator Concept
12	Pitch Drive Control System - Functional Schematic
13	Pitch Drive Control Electronics - Interconnection Diagram
14	Translational Drive Control System - Functional Schematic
15	Translational Drive Control System - Interconnection Diagram
16	Relay Interface Circuit - Schematic
17	Microcomputer Interface Circuit - Single Channel Schematic
18	Selection of Motor Characteristics
19	Position Potentiometer Amplified Circuit

LIST OF FIGURES (CONTINUED)

<u>#</u>	<u>TITLE</u>
20	Pitch Oscillator Performance, Constant Rate Motion, Low to Moderate Frequencies
21	Pitch Oscillator Performance, Constant Rate Motion, High Frequency (Typical)
22	Pitch Performance Comparison, Constant Rate Motion
23	Pitch Oscillation Performance, Constant Acceleration
24	Pitch Performance Comparison, Constant Acceleration
25	Translational Oscillator Performance, Constant Rate Motion
26	Translational Drive Performance - Tunnel Off, Constant Rate Motion
27	Translational Drive Performance - Tunnel Off, Constant Acceleration Performance
28	Combined Drive Performance - Illustration at High Frequency
29	Pitch Axis Performance Map - Streaming Conditions

I. Introduction

Recent interest in the complex flow separation phenomena which have been observed to accompany airfoil dynamic stall has precipitated a requirement to generate arbitrary but controlled model motions in the laboratory environment. Numerous previous research efforts (e.g., see References 1-5) have been limited to examining the effects of nominally harmonic (sinusoidal) oscillations due, in part, to the complexity involved in the design and fabrication of a more general purpose device. Recent improvements in the response characteristics of advanced hybrid servo systems and, independently, the development of the low cost microcomputer for control applications have been exploited to produce a mechanism which possesses heretofore unrealized flexibility in achieving a wide range of motion alternatives.

This report describes and discusses the design and operation of a prototype, multi-purpose oscillation apparatus capable of providing simultaneous, independent motions of an airfoil (or other) model in two degrees of freedom. In combination with the measurement techniques discussed later, the concept affords a high degree of cycle-to-cycle repeatability and a potential to generate any of a virtually infinite variety of simultaneous complex motions in both rotation and translation.

The specific system was designed and constructed for advanced dynamic stall studies at the Frank J. Seiler Research Laboratory and permitted controlled repetitive motions of several small airfoil models (6- to 8-inch chord) in both pitch and translation. Depending on the orientation of the test apparatus, translational motion could be produced in either the free-stream or cross-stream directions. The entire apparatus was located adjacent to and just outside of the 2 ft x 3 ft subsonic wind tunnel test section allowing only the model to be exposed to the air stream through a slot in the test section floor.

The oscillator system is functionally composed of four elements: (1) the Motion Transfer Apparatus, (2) the Model and its interface collar, (3) Dual Hybrid Servo Drive Units and (4) a Microcomputer Control System. These elements are depicted schematically in Figure 1. The Motion Transfer Apparatus is a device constructed from aluminum and steel components which serves to transform shaft displacements from the drive motors to desired model motions. The model is fastened to this apparatus through a coupling on the rotational (pitch) drive yoke. The Servo Drive Units are complex feedback controlled positioning systems capable of accurate instantaneous rate control which independently provide power to the Motion Transfer Apparatus in both degrees of freedom. Pulse width modulation techniques are employed in these units to maximize power transfer rate and, therefore, optimize overall system response. The Microcomputer Control System provides a preprogrammed series of pulses to the Servo Drive Units which then effect the desired displacements. Both units are simultaneously controlled by the same microcomputer CPU.

Each of the elements briefly described above is the subject of a separate section of this report. While these elements and their integration remain the primary focus of this document, the role of the entire mechanism in the overall experimental arrangement is also addressed, especially its relationship to the host data acquisition minicomputer which functions as the experiment's central control manager. The performance characteristics of the overall system when subjected to various test conditions are also discussed.

II. Mechanical Design

A. Motion Transfer Apparatus

Perhaps the least complex of the sub-systems mentioned in the preceding section is the Motion Transfer Apparatus - a mechanical assembly which transfers kinetic energy from the drive motors to the wind tunnel model. This device consists of an aluminum frame on which the various drive train components are mounted and interconnected. The entire assembly is supported by a steel mainframe fabricated from heavy gauge angle sections and provided with casters for portability when not in use. During operation, the unit is located outside of and below the wind tunnel test section so that only the model protrudes into the airstream. The complete apparatus is depicted in Figure 2.

The drive system is configured in a dual yoke arrangement which provides uncoupled motions in rotation (pitching motion, in this case) and translation. The pitch drive assembly, including the pitch motor, is "piggy-backed" on the translational drive unit. In this configuration, a much lower power requirement results for the pitch drive motor compared to the translational drive unit. Both drives are designed to provide minimal mechanical amplification factors for maximum dynamic response.

B. Pitch Drive Assembly

Rotational, or pitch, motion is generated through the pitch yoke sub-assembly which is depicted schematically in Figure 3. Angular displacement of the drive motor shaft is first converted to linear displacement of the yoke assembly through a coupler device which connects the motor flywheel to the yoke cross-rod through a ball bushing encasement which is free to slide along the cross-rod. A cylindrical bearing mounted in the coupler device is mated to an interconnecting pin which protrudes from an off-center location

on the flywheel surface. As the flywheel turns, the yoke is displaced in the x-direction with alignment maintained by four support ball bushings. This linear motion is then reconverted into angular motion of the model attachment shaft through a rack and spur gear assembly. Because of severe dynamic motion requirements, the gear and rack were fabricated from steel with coarse profiles for added strength. All components of the drive apparatus are constructed from heavy duty materials in a configuration optimized for high mechanical strength and stiffness but with a light overall weight.

The resulting mechanical amplification of this assembly is then unity; that is, one complete revolution of the motor shaft coincides with one cycle of model rotation from the initial angle (α_0), through the maximum angle, and back again. A computation of the mechanical transfer function which relates the instantaneous model pitch angle (α) to the motor shaft displacement angle (θ_1) results in the following relationship -

$$\alpha - \alpha_0 = \frac{r_2}{r_1} (1 - \cos \theta_1) \quad (1a)$$

or, alternatively -

$$\theta_1 = \cos^{-1} \left[1 - \frac{r_1}{r_2} (\alpha - \alpha_0) \right] \quad (1b)$$

where

r_1 = spur gear pitch radius

and, r_2 = flywheel attachment radius.

The maximum pitch angle which could be attained is observed to be a function of the flywheel and gear radii, namely,

$$\alpha_{\max} = \alpha_0 + 2 \frac{r_2}{r_1}$$

Although the spur gear geometry was fixed in the design, the effective flywheel radius could be altered to change the value of α_{\max} . The flywheel interconnecting pin is actually fabricated as part of an eccentric cam which is flush mounted in the flywheel. The cam can be rotated through a half-circle providing a wide range of possible values of r_2 , and, thus α_{\max} . After a location is selected, the cam is locked into position for the subsequent test.

The flywheel is constructed from solid aluminum and serves several purposes. It is employed to provide a measure of dynamic balance for the drive system, especially at high speeds. It also possesses sufficient mass to act as a 'smoothing' agent to reduce erratic motion during periods of high acceleration and deceleration.

The mainframe on which the various components are mounted is also used to support the drive motor itself. Two 'U'-shaped braces provide a friction fit capable of easily restraining the motor and flywheel while also functioning as a means for adjusting the motor reference position.

The pitch drive is powered by a high response, DC servo motor of permanent magnet design (Control Systems Research Model No. SM 708-2). The physical dimensions of the unit are shown in the diagram of Figure 4. The package contains an integral position feedback transducer consisting of multiple inductor coils. The unit is accurate to within 0.15 degrees of shaft rotation. The unit is capable of generating up to 50 inch-pounds (5.6 N-m) of torque at 700 rpm. Peak output power of the device is .66 HP (492 watts). The unit weighs 11.5 lb.

The pitch oscillator assembly described in the preceding paragraphs is structurally designed to generate large amplitude ($\pm 40^\circ$) angular oscillations at frequencies to 7 Hz. Anharmonic operating conditions can usually be employed

to provide less severe loading at even higher instantaneous rotation rates - a subject which is discussed below.

C. Model and Model Interface

At this point, it is appropriate to briefly describe the model interface design since it is coupled directly to the pitch drive assembly. The spur gear mentioned above is permanently attached to the hollow model support shaft which is fastened to the lower portion of the mainframe by two alignment bearings (see side view, Figure 3). The model is coupled to this shaft through a 'tang' which protrudes from the base of the model. The tang was fabricated to be inserted into the upper opening of the support shaft and is held in place with recessed set screws. The tang possesses an oblong cross-section and is hollow to allow for the passage of transducer wires from the model's interior to outside electronic signal conditioning instrumentation. A sketch depicting the model mount arrangement is provided in Figure 5.

The initial model to be employed with the oscillator system was an aluminum airfoil having a NACA 0012 cross-section and a rectangular planform of 14 inch span (35.6 cm) and 6 inch chord (15.2 cm). The shape was fabricated from three solid aluminum pieces and excavated to provide interior mounting locations for nineteen (19) miniature piezoresistive pressure transducers (see Figure 6). Short pieces of pliable tubing were used to interconnect the transducer heads with small brass tubes which extended to the model's upper and lower surfaces. This arrangement was necessitated by the small size of the model which precluded flush mounting of any of the transducers with the model's exterior surfaces. Although the installation resulted in a somewhat reduced transducer frequency response, the upper rolloff frequency of each pressure measurement unit was maintained at an acceptable level.

D. Translational Drive Assembly

The entire pitch oscillation mechanism, including the model and the drive motor, is mounted directly to the translational drive yoke assembly. This unit is shown in Figure 7 which also depicts the relative location of the pitch oscillator components.

The mechanical operation of the translation drive train is functionally similar to that of the pitch assembly. Again, flywheel rotation is converted into linear motion through a bearing which couples the flywheel cam to the ball bushing encasement which is free to slide along the yoke cross-rod. The linear displacement (Δx) can be related to the flywheel rotation angle (θ_2) through the following expression -

$$\Delta x = r_3 (1 - \cos \theta_2) \quad (2a)$$

or, alternatively -

$$\theta_2 = \cos^{-1} \left[1 - \frac{\Delta x}{r_3} \right] \quad (2b)$$

where -

r_3 = flywheel attachment radius, translational assembly.

The maximum range of motion is regulated solely by the flywheel diameter in this case. Enlarging the flywheel will provide an increased translational range, but the increased radius will serve to decrease overall acceleration/deceleration capability of the system. The design of the flywheel must, therefore, compromise the conflicting requirements of maximum displacement, high system inertia for smooth constant speed operation, and optimum dynamic response.

The structural requirements of the translation apparatus are severe due to the added inertial resistance provided by the 'piggy-backed' pitch assembly.

As a result, much larger components were used in the construction of this unit including, for example, one-inch diameter rods to support the yoke frame. Every effort was made during the initial design and fabrication to minimize the weight of the moving assembly without compromising requisite structural integrity. The net mass of the complete translational yoke and pitch assembly after all modifications were completed was fixed at 24.9 kg (55 lb) with the NACA 0012 airfoil model installed.

An obvious consequence of the dual yoke design approach described above is the large power requirement for the translational drive stage compared to that for the pitch mechanics. The mechanical performance requirements were ambitiously defined to provide a capability for large amplitude translational oscillations (12 inches, total travel) at a high steady state frequency (3 Hz). The resulting structural design was thought to strike a good balance between maximized performance goals and necessary safety considerations.

To obtain reasonable dynamic performance, a 5 HP, DC motor (L186AT frame) is employed with a regenerative drive power source (Control Systems Research, "Systrol" Model 4200AP). The maximum motor speed is rated at 1750 rpm. To provide necessary torque over the desired operating range, a 10:1 gear reduction stage (Morse, Model 35GCV10) is coupled between the motor drive shaft and the flywheel.

E. Facility Interface

The combined drive assemblies are mounted on a rigid steel frame which is braced with heavy cross members for added stiffness. Four retractable legs constructed from heavy steel angle sections with welded steel 'feet' are anchored to the concrete floor beneath the wind tunnel during operation. When not in use, the entire structure can be removed on its four heavy duty casters by retracting the legs while the frame is supported by jacks. The

mainframe also serves as the primary support for the translational drive motor and gearbox.

Available access to the wind tunnel test section is severely limited restricting the range of possible model mounting schemes. It was for these reasons that the apparatus was designed to provide a model attachment point through a removable portion of the test section floor (Figure 8).

The model attachment shaft coupled to the pitch drive assembly protrudes into the test section through a slot which is cut in the removable floor panel. The slot is oriented in the freestream direction and is of sufficient length to accommodate the maximum extent of translational motion in that direction. It should be noted that the oscillation mechanism was designed to alternatively permit "plunging" motions by rotating the entire apparatus through 90 degrees. In that case, a new floor panel with a slot orthogonal to the freestream direction would have to be constructed.

To prevent leakage near the base of the model and over the remainder of the slotted region, a two-piece neoprene seal was developed. Shown in cross-section in Figure 9, the two stiffened strips of material were overlapped to form a "V"-configuration which was self-sealing except at the model support shaft entrance point. The material stiffness was varied on a trial and error basis to provide the best seal around the model support shaft without sacrificing performance in the open groove region. To prevent possible effects of leakage during actual model tests, and to isolate the airfoil from unwanted wind tunnel wall boundary layer effects, plexiglass endplates were devised for use with the airfoil model described above.

III. Servo-Drive Electronics

The selection of a suitable drive concept to power the two oscillator stages was severely impacted by two demanding performance requirements, namely, (1) maximization of system dynamic response, and (2) the selectable variation of the time histories of the motion parameters, $\alpha(t)$ and $x(t)$. The first of these is attainable through the application of closed loop control techniques. The latter requirement, it was believed, could best be satisfied through the use of real time computer control. Ultimately, both requirements were met through the implementation of these concepts using a device known as a "servo-translator."

It is useful to briefly discuss the operation of a servo system which utilizes both velocity and position feedback. Such a mechanism is shown schematically in Figure 10. As shown, the input voltage to the servo-controller is a "velocity command" which is instantaneously and continuously compared to the velocity feedback signal (tachometer voltage). The difference, the velocity-error voltage, is greatly amplified by the preamplifier and applied to the power amplifier to command motor current. The current generates torque, which, in turn, alters the motor speed to reduce the velocity error voltage. Thus, the servo-controller is always trying to reduce the velocity error to zero.

The position feedback loop controls the position in the same manner that the servo-controller controls speed. A position command generated by an external source is compared with the position feedback signal provided by a linear feedback transducer sensitive to position. The difference, or position-error signal, is amplified to generate the velocity command.

The "servo-translator," mentioned previously, is a device similar to the one just discussed which employs both velocity and position feedback to

provide accurate motion control. The significant difference is the unique design of the input stage which is shown schematically in Figure 11. Closed loop position control is provided by a device termed an Absolute Digital Translator Subtractor* (ADTS) which accepts command information in the form of serial data pulses. Pulse information is compared with a feedback signal from a non-pulse counting type of transducer (a resolver) to close the loop. This design increases noise immunity since the requirement for encoders or other pulse counting feedback circuits is eliminated. Errors due to 'accumulation' associated with these techniques are also eliminated.

The operating system which results is controlled in real time by the incoming command pulse train. Each pulse received will cause the motor to move one increment in the selected direction, and the rate at which the pulses are received determines the instantaneous motor speed. The resolution, or size of an angular increment, is regulated in the design of the ADTS stage in the servo-translator. Input pulses can be generated through a number of techniques including the output of a digital computer.

It is instructive to briefly discuss the operation of the "resolver" - an analog position transducer employed in conjunction with the ADTS. The unit is brushless and utilizes a rotary transformer principle. It contains three (3) inductive elements - windings labeled as (a) Reference, (b) Sine, and (c) Cosine. The reference winding is located on the rotary portion (Rotor) of the resolver while the Sine and Cosine windings are located on the stationary section (Stator). The Reference winding is excited with a 2.5 kHz sinusoidal reference signal provided from the servo-translator unit. With different positions of the rotor, the Sine and Cosine windings will exhibit different

*Patent Applied For, Control Systems Research Corporation.

coupling factors. The Sine and Cosine signals are fed into the ADTS which generates a digital command signal proportional to the sine of the difference between the command angle and the actual Resolver (position transducer shaft) angle.

The diverse power requirements of the two oscillator stages governed the selection of the type of power amplifier employed in the two cases. A dual-state, pulse width modulation (PWM) technique is used to provide rapid power transfer to the pitch drive motor. A discussion of this concept and its advantages in high speed applications can be found in Reference 6. Because of its substantially larger size and capacity, the translation drive motor is equipped with a more conventional SCR power supply (Control Systems Research, Systrol Model 4200AP).

A complete schematic of the pitch drive electronics including computer control elements is provided in Figure 12. A detailed interconnection diagram is shown in Figure 13. The CSR Model ST-70J-2 Servo Translator is the heart of the closed loop system. The unit is equipped with a resolution of 1000 steps per revolution which equates to a motor displacement resolution of 0.36 degrees or a model pitch angle resolution of 0.21 degrees in the worst case with maximum amplitude cam adjustment. This factor provided for maximum resolution and "smoothing" of motion at high speeds consistent with the maximum output pulse rate capability of the computer. A digital display module (CSR Model IA-04) is coupled directly to the servo-translator to monitor displacement repeatability and possible errors incurred from randomly dropped bits. The IPS-3 direct current power supply provides power to the drive motor through the servo power amplifier card. This unit is rated to deliver 15 amps continuous or 45 amps peak during normal operation.

The translational drive electronics are depicted schematically in Figure 14 with a detailed interconnection diagram provided in Figure 15. The system is functionally similar except for the power source. A relay interface panel (shown in detail in Figure 16) is required to provide proper sequencing of field and armature signals during power up and power down operations. Additional "enable" circuits are provided for added safety during the operation of this high power system. Note that the resolver is located on the output shaft of the gearbox. The resolution of the translational stage is set at 2500 steps per flywheel revolution providing 0.015 inches maximum resolution in unidirectional linear travel with the cam adjusted for maximum travel.

A common feature of both drive systems is a limited capability for 'front panel' control which is hard-wired and does not require a separate computer. The rotation direction can be altered by a polarity control on the panel. A constant rate pulse train provided by an internal oscillator in the servo translator and whose level is regulated by a potentiometer can be employed to 'JOG' the system during installation, alignment and during servo system tuning.

The 'HOME' position is a designated reference location for each resolver determined by the alignment of its rotor and stator. This position is adjusted by rotating the resolver case to any desired preset value. A 'GO HOME' command provided through a separate pulse input can be generated either from the computer or front panel to return the system to the reference position at the 'JOG' speed.

Only the serial data pulse inputs and respective 'GO HOME' commands have been implemented through computer control in the present configuration.

IV. Computer Command System

A. Pulse Train Requirements

The choice of a suitable motion control computer was dictated primarily by the nature of the pulse train which must be produced as an input for the servo-translator. In the present case, this choice was also affected by the necessity to produce two independent drive signals simultaneously. An additional factor which complicated the pulse rate requirement was the non-linear character of the mechanical transfer functions (equations (1) and (2)).

For a given drive system, the net number of pulses applied for unidirectional motion can be related to the flywheel angular displacement as follows -

$$n = K \cdot \Delta\theta \quad (3)$$

where -

n = number of pulses generated

K = 'resolution' of the system (steps per degree)

At this point, it is useful to discuss the concept of 'HOME' or zero reference position. This location is found when the resolver shaft and stator are aligned to produce a 'null' reference signal. If the home position of the resolver is aligned with the x-axis (Figure 4 or 7), the displacement angle, $\Delta\theta$, is equivalent to the absolute angle, θ . Since, realistically, there is always some degree of misalignment, it is appropriate to replace the angle (θ_1 or θ_2) in equations (1) and (2) with an expression which includes the reference offset angle, θ_r , namely -

$$\theta_i = \theta_{s_i} + \theta_{r_i} \quad (4)$$

where -

i = index, denotes the appropriate stage.

The pulse rate can be computed easily from equation (3) as -

$$\dot{n} \equiv \frac{dn}{dt} = K\dot{\theta}_s \quad (5)$$

For the pitch drive assembly, this can be expanded to obtain -

$$\dot{n}_1(t) = K_1 \cdot \frac{r_1}{r_2} \cdot \frac{\dot{\alpha}(t)}{\sin [\theta_{s1}(t) + \theta_{r1}]} \quad (6)$$

The corresponding expression for the translational drive system is calculated as -

$$\dot{n}_2(t) = K_2 \cdot \frac{1}{r_3} \cdot \frac{\Delta \dot{x}(t)}{\sin [\theta_{s2}(t) + \theta_{r2}]} \quad (7)$$

Examination of these relationships reveals, for example, that harmonic motion of either drive output (α , or x) can be generated with a constant pulse rate (\dot{n}). To generate a rampwise behavior in time, e.g., $\dot{\alpha}$ or \dot{x} is a constant, requires a non-linear pulse generation scheme.

It should be noted that since the control pulse trains are to be provided through computer software, provision must also be made in programs for acceleration and deceleration control so as not to exceed drive hardware limitations. This is especially important when rapid motion is required, and when operating near 'HOME' or its complement, i.e., when -

$$\theta_s + \theta_r \rightarrow 0 \text{ or } n\pi$$

At the extrema of the cycle, infinite pulse rates are required to maintain constant rate model motions.

B. Hardware

To produce the dual pulse trains required for simultaneous operation of the drive systems, a Digital Equipment Corporation PDP 11/03 microcomputer was chosen for dedicated motion control. The unit was configured with 32

k-bytes random access memory which provided overhead (operating system) and program support.

Control of the two motor drive systems was implemented through a single digital output port using select pins for the various pulse and voltage level command functions (see Figures 13 and 15). Pulses were generated by momentary "togglng" of the voltage at the appropriate output register pin from the low to high state. The timing of the pulses for each control channel was accomplished in software by indexing a 'pointer' through a binary array. Each bit is examined by software as the pointer reaches it resulting in a toggle command to the appropriate output port if a "1" is detected. Bits set to "0" are ignored. Succeeding bits are examined alternately from the two arrays which determine pitch and translational motion. The pointer indexing rate is regulated by the internal computer instruction clock, and, in this manner, a pulse train having a prescribed time history, $n(t)$, can be generated programmatically.

Other register pins can be employed to control other elements of model motion using voltage level variations. For example, the direction of motor rotation could have been changed through a software command to a preselected output pin. This option has not been exercised in the present case, however.

Resulting motion is then a single cycle pattern which can be repeated as many times as required by relocating the pointer to the top of the arrays and restarting the sequencing program.

Due to the high noise environment and long control cables used in the experiment, a two-channel, interface circuit was installed near the servo-translator input to perform pulse shaping and timing regulation. The schematic diagram for a single channel is provided in Figure 17. The DM74121 monostable multivibrator chips are used to provide 'clean' pulses exhibiting rapid rise/

fall rates (less than 1.0 μ sec) and of precise duration (pulse width 10 μ sec, minimum detectable is 5 μ sec). The DM7416 Hex Inverter module is employed to interface complimentary logic schemes of the computer output and servo-translator electronics.

Although the microcomputer system described above was adequate for motion control, the limited memory and lack of storage peripherals severely restricted its use for program development. Since a larger, minicomputer system was available for overall experimental control and data acquisition, a capability was developed to interface the larger machine with the smaller one for transferring task images using a 'down-line load' technique. This simple network allowed for program development and editing in the DEC PDP 11/45 computer system which was equipped with magnetic disk storage capability. The sophisticated operating system of this unit also provided a capability to employ higher order languages such as FORTRAN. After the necessary control program is developed, it can be transferred to the microcomputer via the network link.

During an actual test, the microcomputer is employed as a dedicated motion controller which is slaved to the larger computer. The minicomputer protocol evokes the initiation of prescribed motion through a single command to the microcomputer, and the larger machine subsequently samples data from the various transducers employed in the experiment. Precise timing in the coupled computer interaction is the key to repeatable, phase-locked sampling and accurate ensemble averages of the various data parameters.

C. Software

As of this writing, motion control programs had been developed to implement constant rate (ramp function), constant acceleration or harmonic motions of either or both drive systems including asynchronous initiation. A chart showing the motion selection and control algorithm is provided in Figure 18.

After the 'RUN' command is provided through the microcomputer control terminal, the program queries the user for the desired motion parameters including:

- (1) type of motion for pitch
- (2) type of motion for acceleration
- (3) rate information for both axes (e.g., $\dot{\alpha}$, $\ddot{\alpha}$, or frequency)
- (4) motion initial conditions for constant acceleration (e.g., $\dot{\alpha}_0$ or \dot{x}_0)
- (5) maximum travel limits for both axes
- (6) timed delay for start of motion, if desired

and,

- (7) total time until a 'GO HOME' pulse is generated after motion completion.

The program then calculates the bits in the motion array that must be set to obtain the desired motion. An example for constant acceleration in pitch is illustrative. For this case, the operator inputs the desired pitch acceleration, the initial pitch rate, and the maximum angle of attack desired. Since the time between pulses Δt is the inverse of the pulse rate, $\Delta t = 1/\dot{n}$, equation (6) is used to calculate the time increment. For this calculation, the pitch rate is calculated from the expression -

$$\dot{\alpha}(t) = \ddot{\alpha} \cdot t + \dot{\alpha}_0$$

In this step, any functional form for pitch rate could have been substituted.

The time increment is added to the time total to give the absolute time after motion initiation when a pulse should occur. These absolute time values are then used to determine the sequence of bits to be set in the motion array which will result in incrementing the motor shaft angle when the 'RUN' program is executed.

The calculation of time steps is iterative, involving a repeated computation of instantaneous pitch rate and corresponding time increment until the maximum angle of attack is reached. The program will then branch to a routine which will set the bits in the translational motion array in a similar fashion.

When the bits have been set in both arrays, the unit will idle until a 'START MOTION' pulse command is generated by the minicomputer manager. Once initiated, the slave computer will step through its motion arrays, outputting pulses to the drive electronics. When motion is complete, a 'GO HOME' pulse is generated to both drives, returning them to the 'HOME' position. The motion can then be precisely repeated, on command, as many times as necessary. The program is terminated by another command from the host minicomputer.

V. Performance

Preliminary motion control experiments were conducted using the integrated oscillator mechanics and electronic control components to evaluate overall system performance. The tests were structured to address two areas of concern, namely, (1) the comparison of actual motion time histories (dynamic response) with "programmed" motion, and (2) the cycle-to-cycle repeatability of preselected motion over a range of performance conditions.

To assess performance, position variables (as functions of time) were measured independently using precision, servo mount potentiometers as linear position transducers. A single turn, precision potentiometer equipped with a small spur gear was interfaced to a rack assembly which was fastened to the movable portion of the pitch yoke. When the wiper of the transducer was interfaced with the DC amplifier shown in Figure 19, the resulting voltage output level was linearly related to yoke position, and, hence, to the instantaneous angle-of-attack. The principal source of error in establishing this relationship, gear-rack backlash, was estimated to be less than 0.05% for unidirectional motions.

A similar arrangement was configured for the translational drive stage using a ten turn, precision potentiometer and an appropriately sized gear. In this case, translational position was measured directly.

Analog position signals were digitized through the LPS-11 analog/digital converter interface available with the PDP 11/45 data acquisition system and stored on disk. Performance tests were conducted under "no flow" conditions for pitch-only, translation-only and combined pitch/translational conditions.

Several actual time histories obtained for a range of pitch rates are displayed in Figures 20 and 21. The data provided in these illustrations represent a request for a constant rate of change in angle-of-attack ($\dot{\alpha}$) from

zero degrees to a prescribed level (α_{\max}) with delay and a subsequent 'RETURN HOME' command at a later time. At low to moderate rates ($10^0/\text{sec} < \dot{\alpha} < 500^0/\text{sec}$), the actual motion time history was quite consistent with the programmed "request." The linear region is observed to extend to α_{\max} with sharp acceleration and deceleration characteristics near motion initiation and termination, respectively. Extensive tests did verify, however, that it was necessary to "tune" the entire system in order to optimize performance and to obtain faithfully reproducible response from test to test, even for the lower oscillation rates. The tuning process included not only adjusting the servo system gain and electronic response for critically damped behavior as might be expected, but also the painstaking alignment of all moving mechanical components to eliminate friction and binding to the maximum extent possible.

At higher frequencies, inherent performance limitations were responsible for varying degrees of degraded motion response. The curve depicted in Figure 21 is representative of this behavior for constant rate motion. The curve has been divided into three regions to facilitate a discussion of the dynamic characteristics.

The initial acceleration is not "instantaneous" in this time scale of motion as is shown in the segment labeled region I. Limitations on acceleration capability resulted from the torque limitations of the motor gearbox system as well as the maximum pulse frequency output of the microcomputer. As previously mentioned, with the yoked drive arrangement employed, more pulses were required to move a finite displacement ($\Delta\alpha$ or Δx) when the yoke was near either end of its range of motion, i.e., during the initial and final portions of the motion cycle. There is even a slight delay in the

onset of motion (no greater than 0.02 sec) which can be attributed to the time response of the electronics and software - a fixed delay time.

The linearity of the constant rate region (II) is observed to be a strong function of the rate itself. From rates in excess of approximately 500 degrees per second to those in excess of 1,100 degrees per second (the maximum attempted), the linear portion of the curve was found to extend from a starting angle (α_1) which was typically fixed at about four degrees (well under the static stall value) to a maximum level (α_2) which was a fractional portion of the maximum actual value. Typically -

$$\alpha_2 \approx 0.88 \alpha_3$$

In this example, $\alpha_2 = 55$ degrees for a programmed maximum of 60 degrees and an actual value, $\alpha_3 = 62$ degrees. It should be noted that the maximum obtainable limit with the internal cam (flywheel) adjusted for maximum radius (r_2 , from equation (1)) was $\alpha_{\max} = 68.3$ degrees. The nonlinearity of this region was typically no worse than 4-5% for the highest rates attainable based on a best linear fit curve.

The deceleration phase (region III) is characterized by an overshoot of the desired termination angle (α_{\max}) followed by a damped oscillation to equilibrium. The extent of the overshoot was fixed at about 3-4% of α_{\max} , but the damping was found to be dependent on the actual rate, $\dot{\alpha}$. This behavior is attributable to the previously described limitations on the maximum frequency and torque capabilities of the system to respond to an "instantaneous" deceleration request.

An item of concern, especially at high programmed rates, is the ability of the drive unit to provide the actual requested rate during the linear segment of motion. The example provided in Figure 21 does appear to indicate a

difference between the 'real' and the 'ideal' rates. These results are summarized for a range of rates in Figure 22. The data represent actual rates measured over the linear region only using a 'best fit' curve. The departure from ideal motion is observed to increase with increasing rate in a slightly nonlinear fashion.

Similar results are provided for the pitch oscillation mechanism for the case of acceleration at constant rate, that is, $\ddot{\alpha} = \text{constant}$, as shown in Figure 23. After the maximum angle has been reached, the level is held until the 'RETURN HOME' command has been provided. These data reveal less overshoot and oscillation during the deceleration part of the motion when compared to the constant rate motion. A comparison of actual versus programmed acceleration is provided in Figure 24 showing a closer adherence to desired performance than that depicted for constant rate motion.

Comparable results are provided for the translational drive stage in Figures 25-27. Performance indicators for this unit are similar to those discussed previously for the pitch mechanism. It must again be noted that the inertial limitations of this unit are much more severe than for the smaller pitch apparatus, and this is reflected in the 'frequency' range depicted in the figures. The maximum translational rate attempted under "no-flow" test conditions for this report was $\dot{x} = 50$ inches per second. The significance of this performance parameter is apparent when it is compared with the minimum streaming velocities to which the model might be subjected. The USAFA subsonic wind tunnel provided test section flow velocities down to 32 feet per second (with special modifications) which results in a typical speed perturbation of approximately 16%.

An issue of equal concern to those mentioned previously is the 'integrity' of resultant motion, or, cycle-to-cycle repeatability. Although the actual

performance of both stages was observed to depart from the programmed parameters, the measured repeatability of the resultant motion was found to be excellent. Even after prolonged periods (> 500 cycles), no deviation in repeated oscillograph traces of the motion time histories was detectable. The overall repeatability of the patterns, irrespective of the type of motion or drive unit, is estimated to be within one-half of one per cent.

Several tests involving simultaneous motion of both stages were conducted to assess possible degradation of motion due to inertial interference effects. Figure 28 illustrates one example of combined motion. In this case, an axial deceleration is coupled with a delayed pitch motion at constant rate. In these tests, no apparent alteration of the independent motions was observed due to the coupling.

Finally, it is useful to discuss the performance 'map' under streaming conditions. A typical result is provided for the pitch drive unit (Figure 29) which shows the envelope of constant "quality" motion as a function of the test section flow velocity. A diagram of this type could also be generated for the translational axis. Of course, this family of curves would be altered if a different model (inertial characteristics) were employed. If other than constant rate motion were considered, the ordinate would have to be redefined to reflect the relevant performance variables.

VI. Summary

An oscillator mechanism which provides complex motions in two degrees-of-freedom has been described. The device, originally designed for the investigation of motion variations in dynamic stall, employs a unique microcomputer-controlled, servo system concept to generate a virtually infinite combination of motion alternatives in simultaneous rotation and translation. A preliminary performance evaluation indicates that the apparatus is capable of generating relatively large amplitude dynamic motions at high frequencies. Performance limitations have also been documented.

References

1. McAlister, K. W., Carr, L. W., and McCroskey, W. J., "Dynamic Stall Experiments on the NACA 0012 Airfoil," NASA Technical Paper 1100, January 1978, 162 pages.
2. Parker, A. G., "Force and Pressure Measurements on an Airfoil Oscillating Through Stall," Journal of Aircraft, Vol. 13, No. 10, October 1976, pp. 823-827.
3. St. Hilaire, A. O., Carta, F. O., Fink, M. R., and Jepson, W. D., "The Influence of Sweep on the Aerodynamic Loading of an Oscillating NACA 0012 Airfoil," NASA Contractor Report 3092, May 1979.
4. Francis, M. S., Keesee, J. E., Lang, J. D., Sparks, G. W., and Sisson, G. E., "Aerodynamic Characteristics of an Unsteady Separated Flow," AIAA Journal, Vol. 17, No. 12, December 1979, pp. 1332-1339.
5. Viets, H., Piatt, M., and Ball, M., "Boundary Layer Control by Unsteady Vortex Generation," Proceedings - Symposium on Aerodynamics of Transportation (ASME), June 1979.
6. Kechbauch, Thomas J., "The Servodrive - it really does make a difference," Tooling and Production Magazine, December 1976.

Acknowledgements

The authors wish to gratefully acknowledge the painstaking efforts of Mr. Carl Geddes, whose talent and expertise are responsible for the fabrication and successful operation of the two degree-of-freedom oscillation mechanism. Dr. (then, Captain) Stephen Batill and Mr. (then, Lieutenant) Paul Duesing are to be especially commended for their contributions to the complex mechanical design of the apparatus. Captain James Lind assisted greatly in the development of the computer interface and control software.

The oscillator mechanism was constructed as part of a sponsored research effort supported by the Frank J. Seiler Research Laboratory. Additional support was also provided by the Flight Dynamics Laboratory of the Air Force Wright Aeronautical Laboratories.

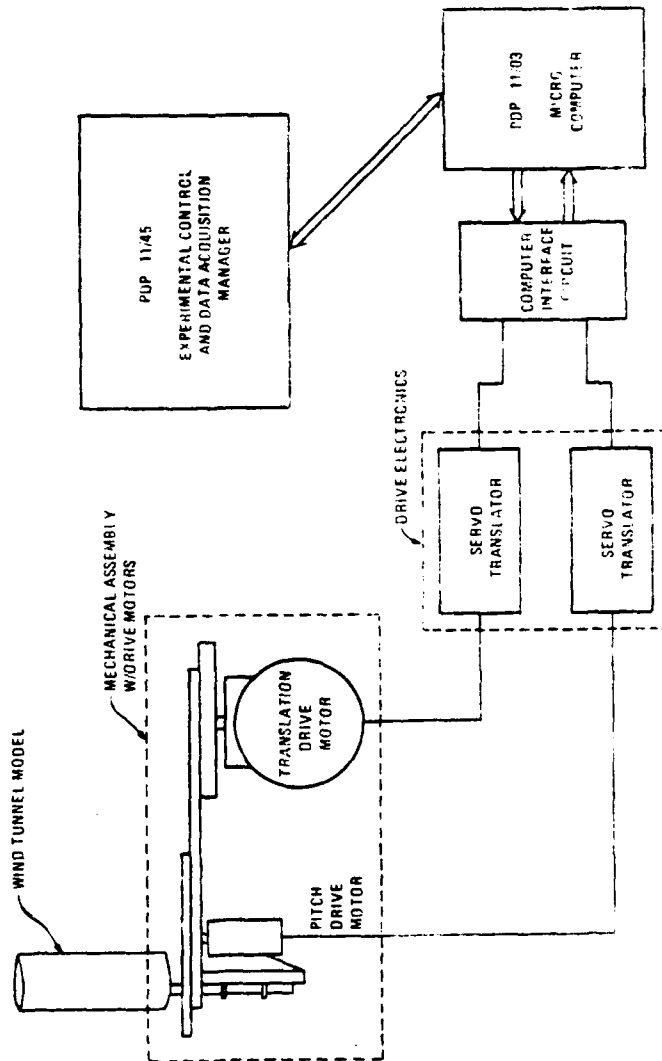


Figure 1. Two-Degree-of-Freedom Apparatus, Functional Schematic

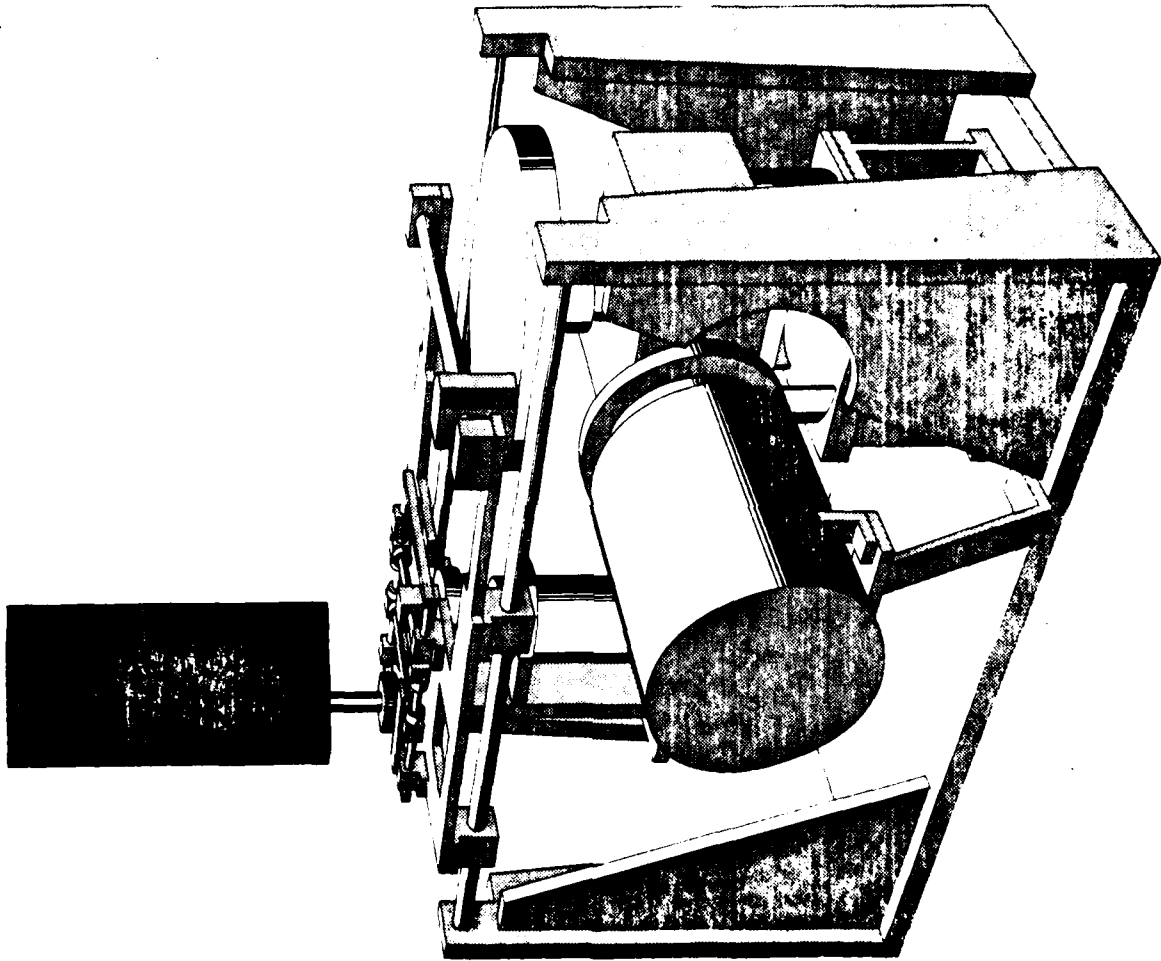


Figure 2. Mechanical Oscillation Assembly

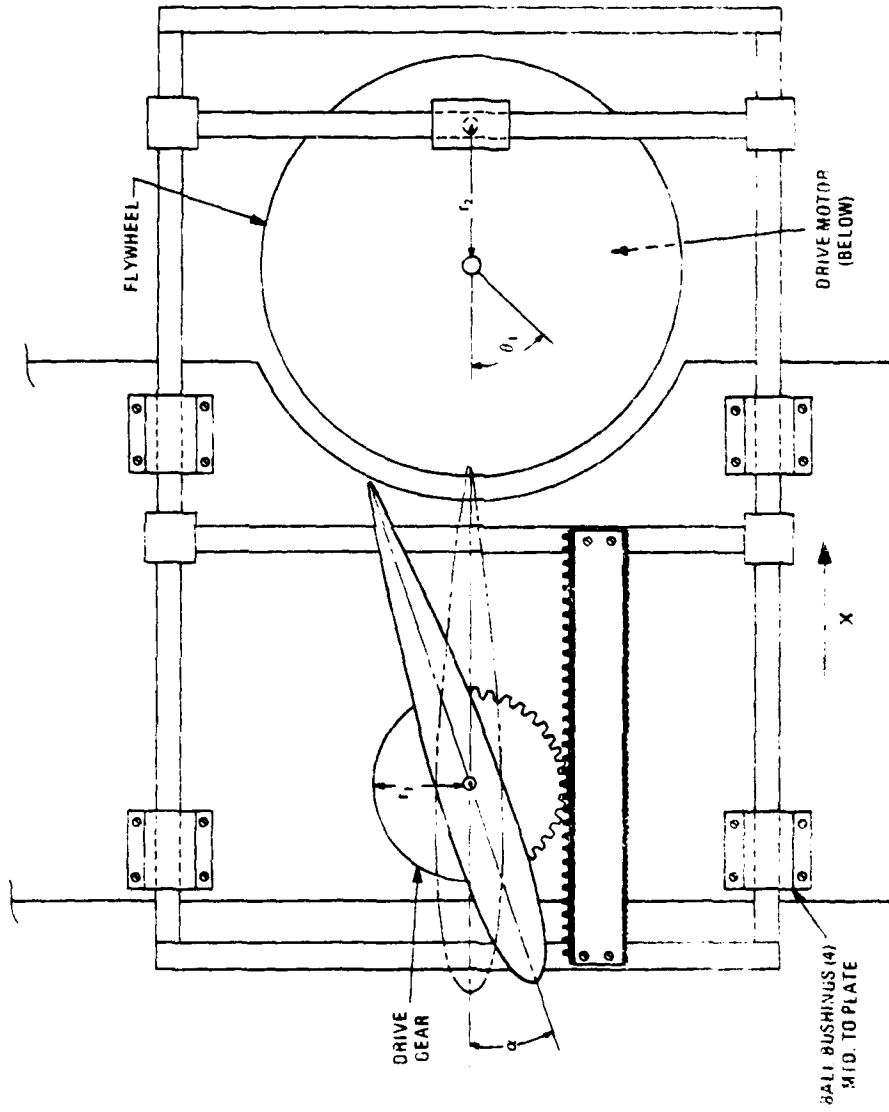
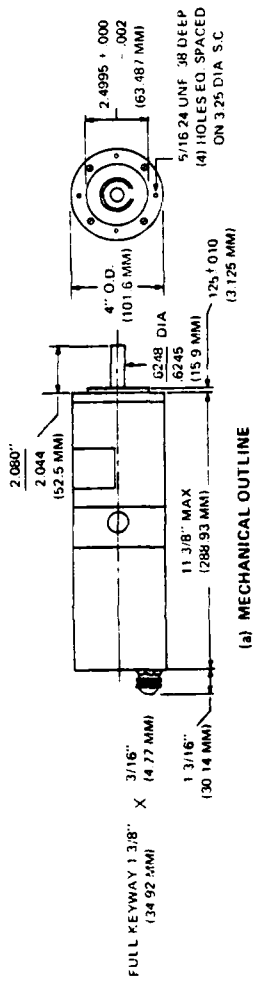
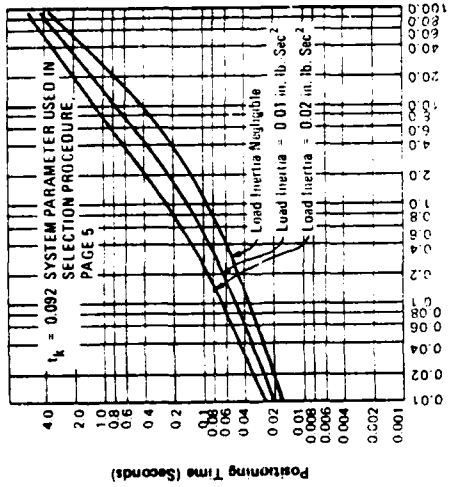


Figure 3. Pitch Yoke Sub-Assembly

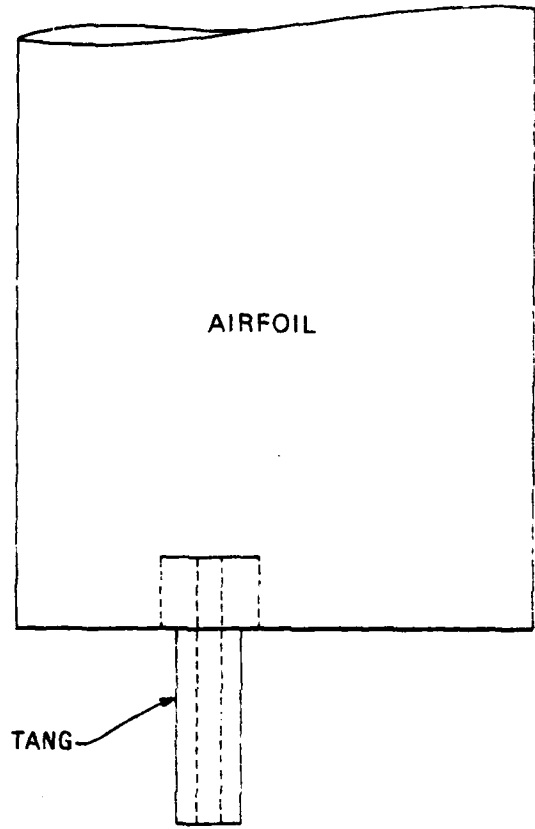


(a) MECHANICAL OUTLINE



(b) PERFORMANCE WITH TYPE 2 MOTOR DRIVER

Figure 5. SM 708 Series Motor - Description



Side View



Bottom View

Figure 5. Model Mounting Detail

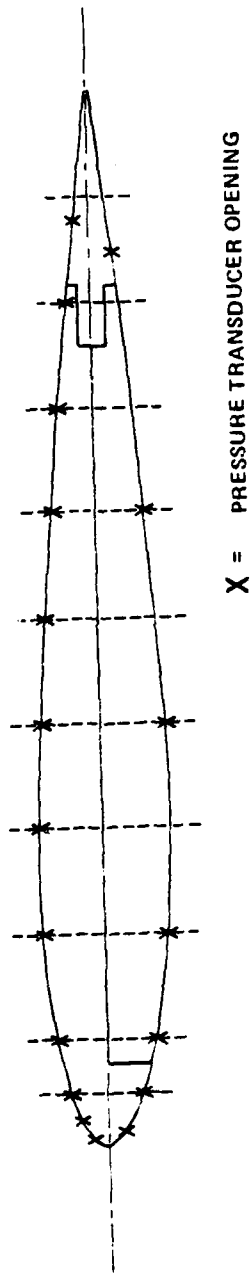


Figure 6. NACA 0012 Airfoil Model and Instrumentation

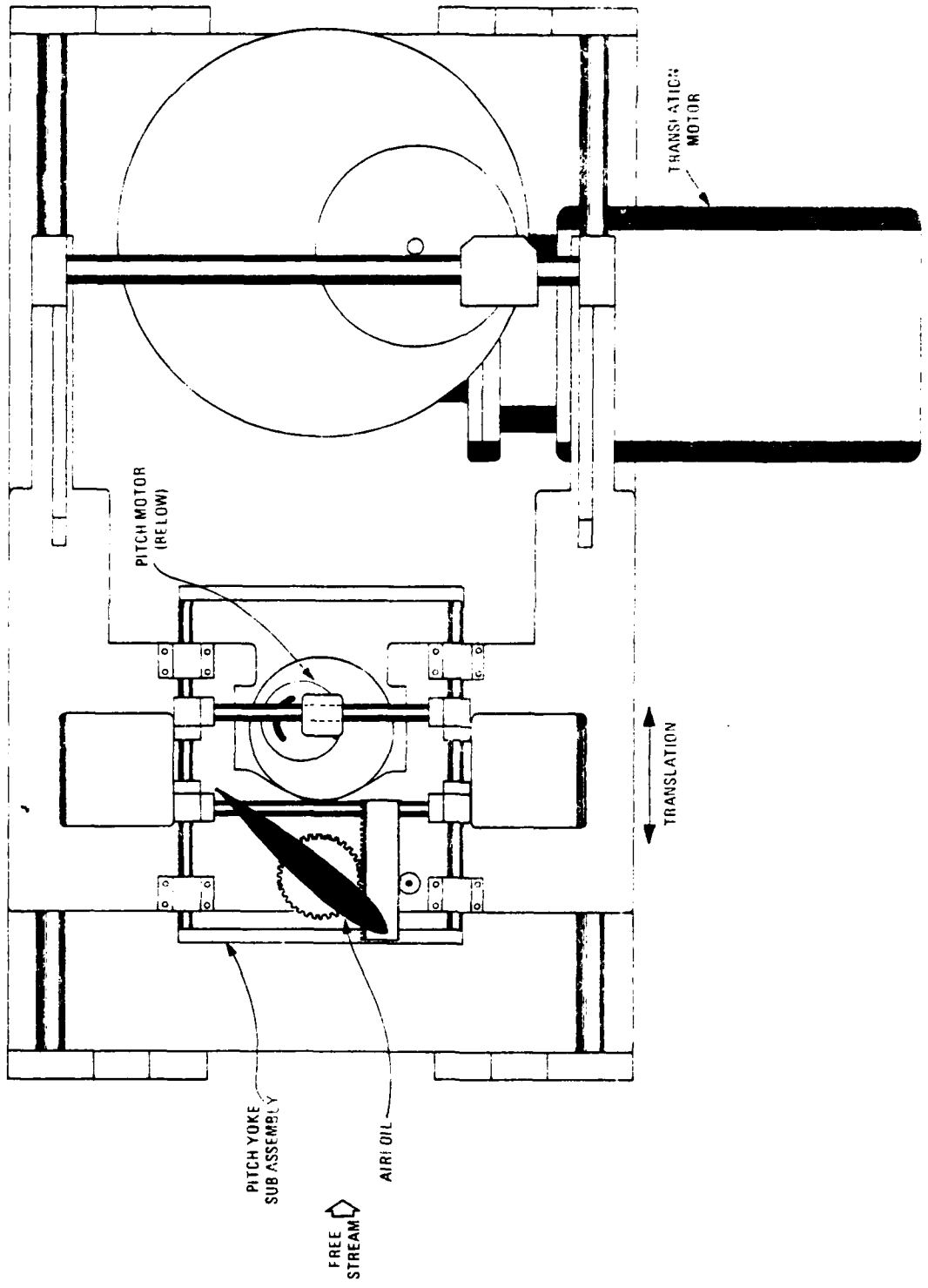


Figure 7. Translation Assembly

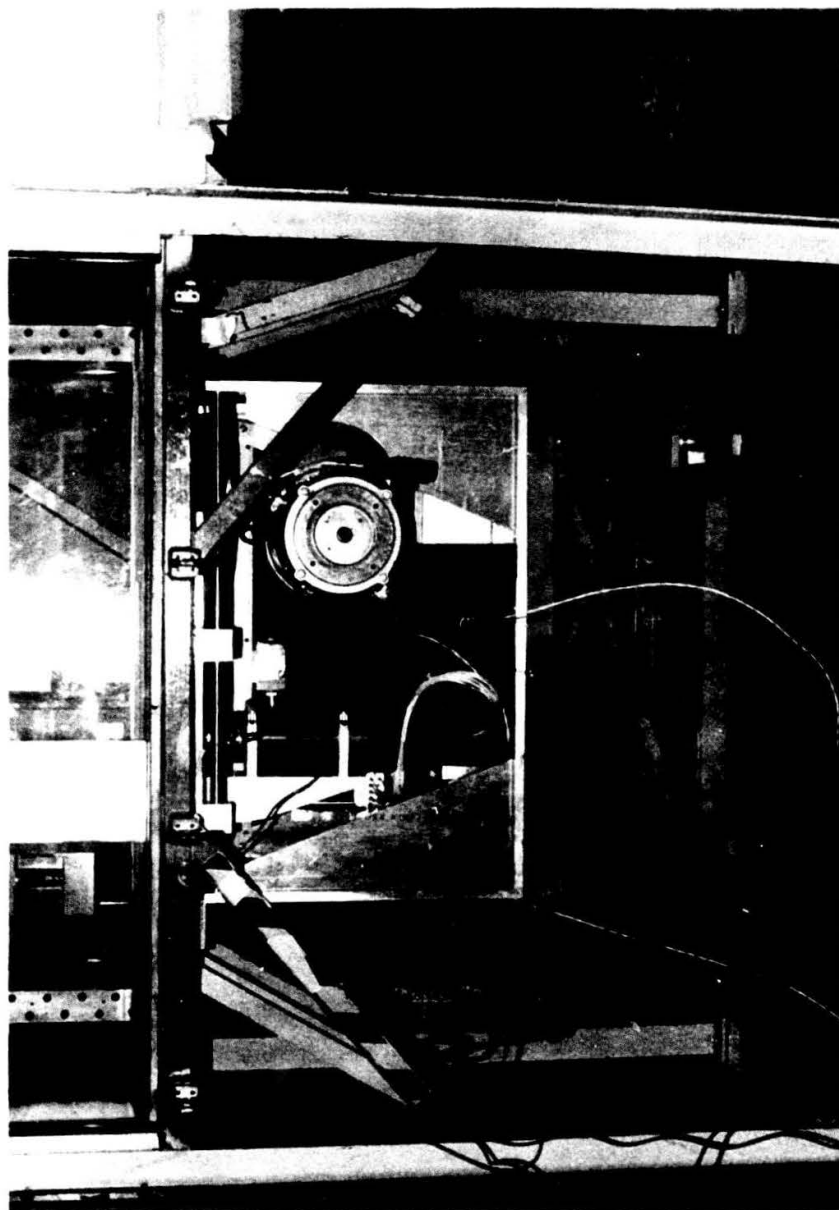
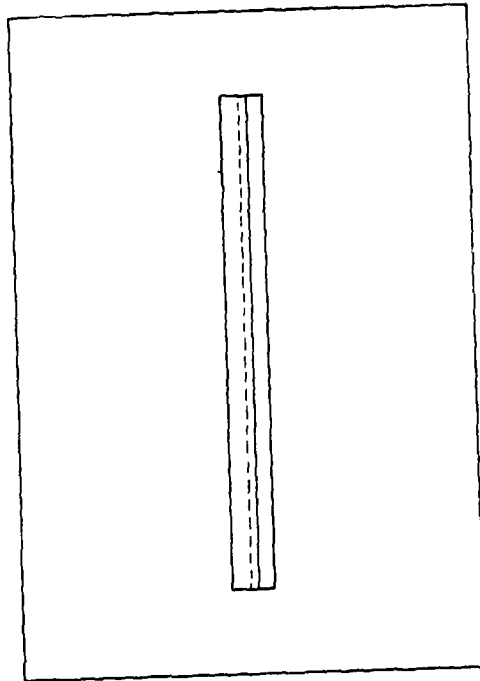
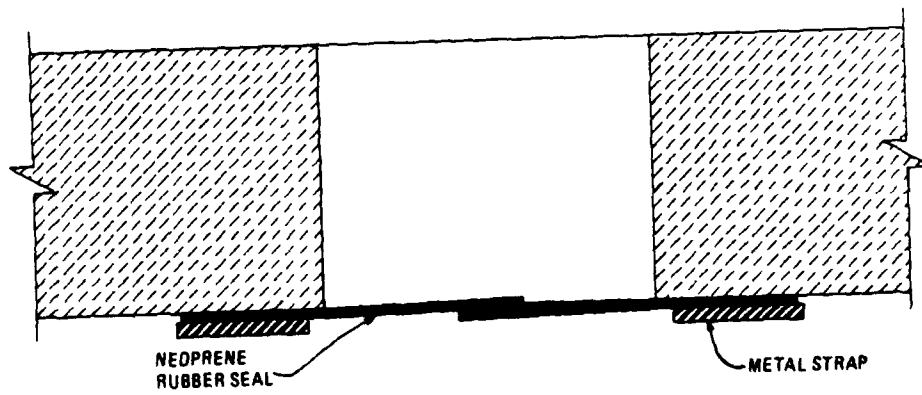


Figure 8. Experiment Installed in USAFA 2 ft x 3 ft Subsonic Wind Tunnel



Top View



NEOPRENE
RUBBER SEAL

METAL STRAP

Sectional End View

Figure 9. Neoprene Slot Seal

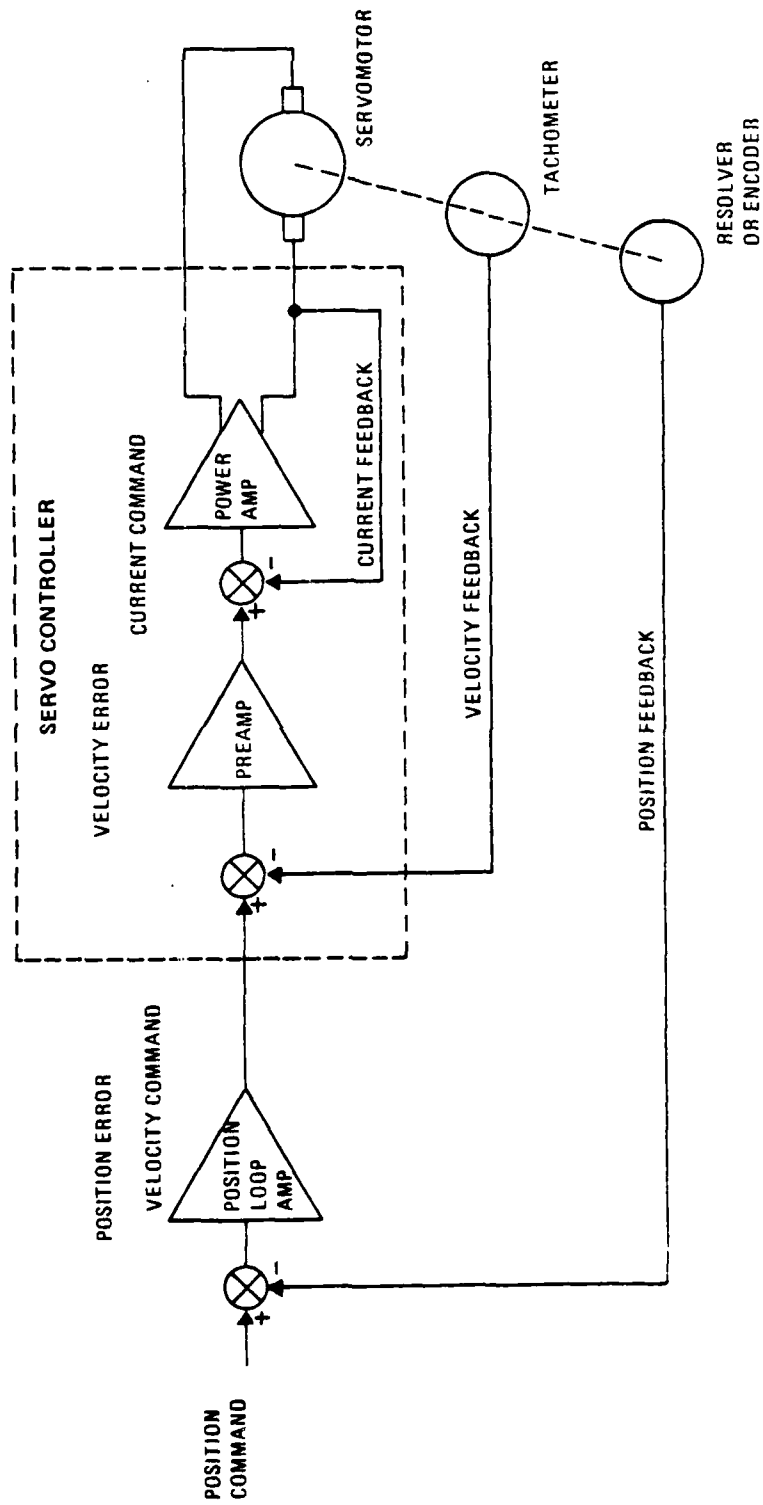


Figure 10. Servo Drive Electronics - Schematic

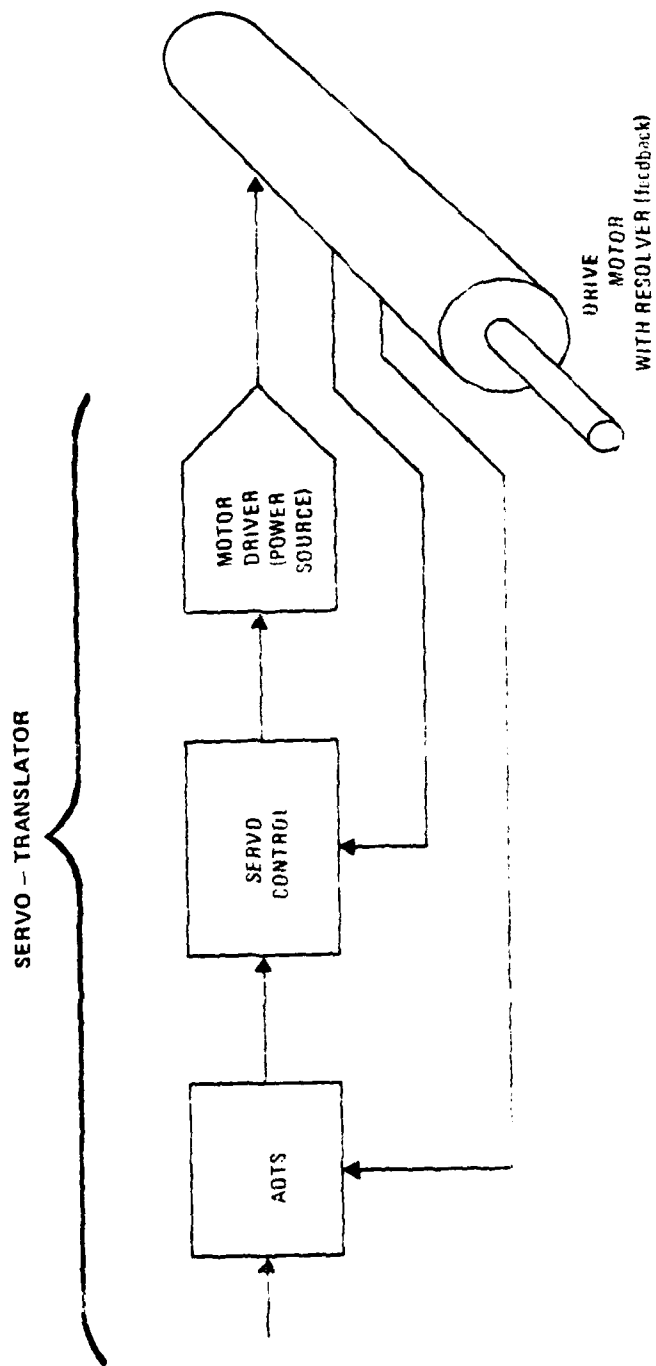


Figure 11. Servo Translator Concept

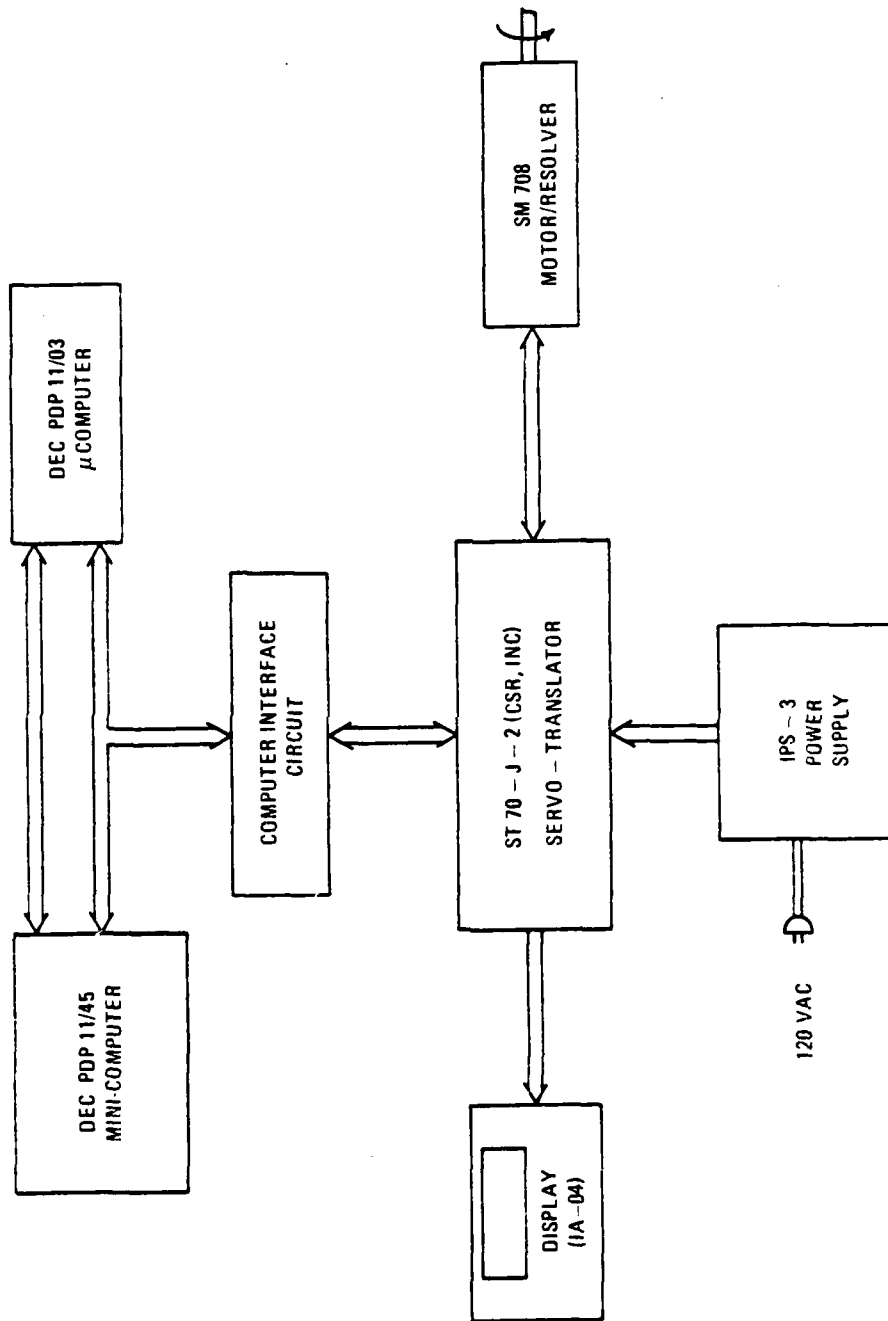


Figure 12. Pitch Drive Control System - Functional Schematic

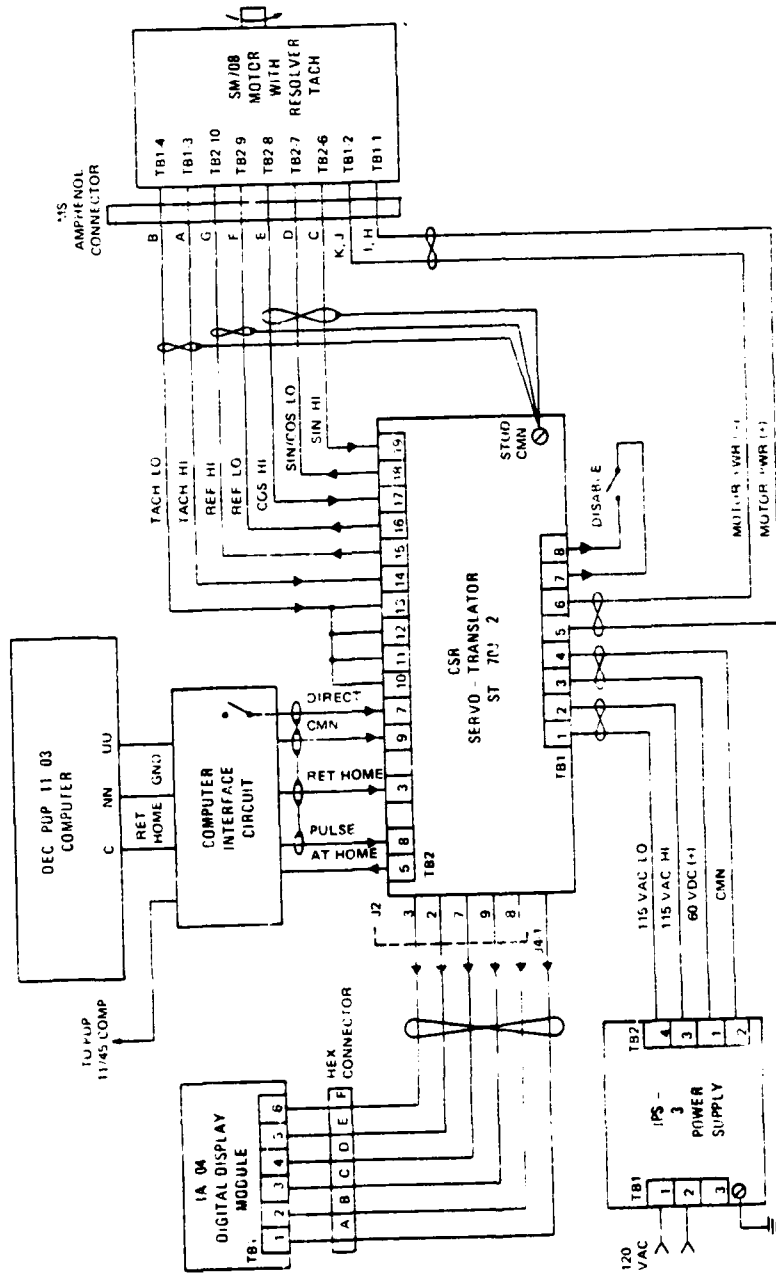


Figure 13. Pitch Drive Control Electronics - Interconnection Diagram

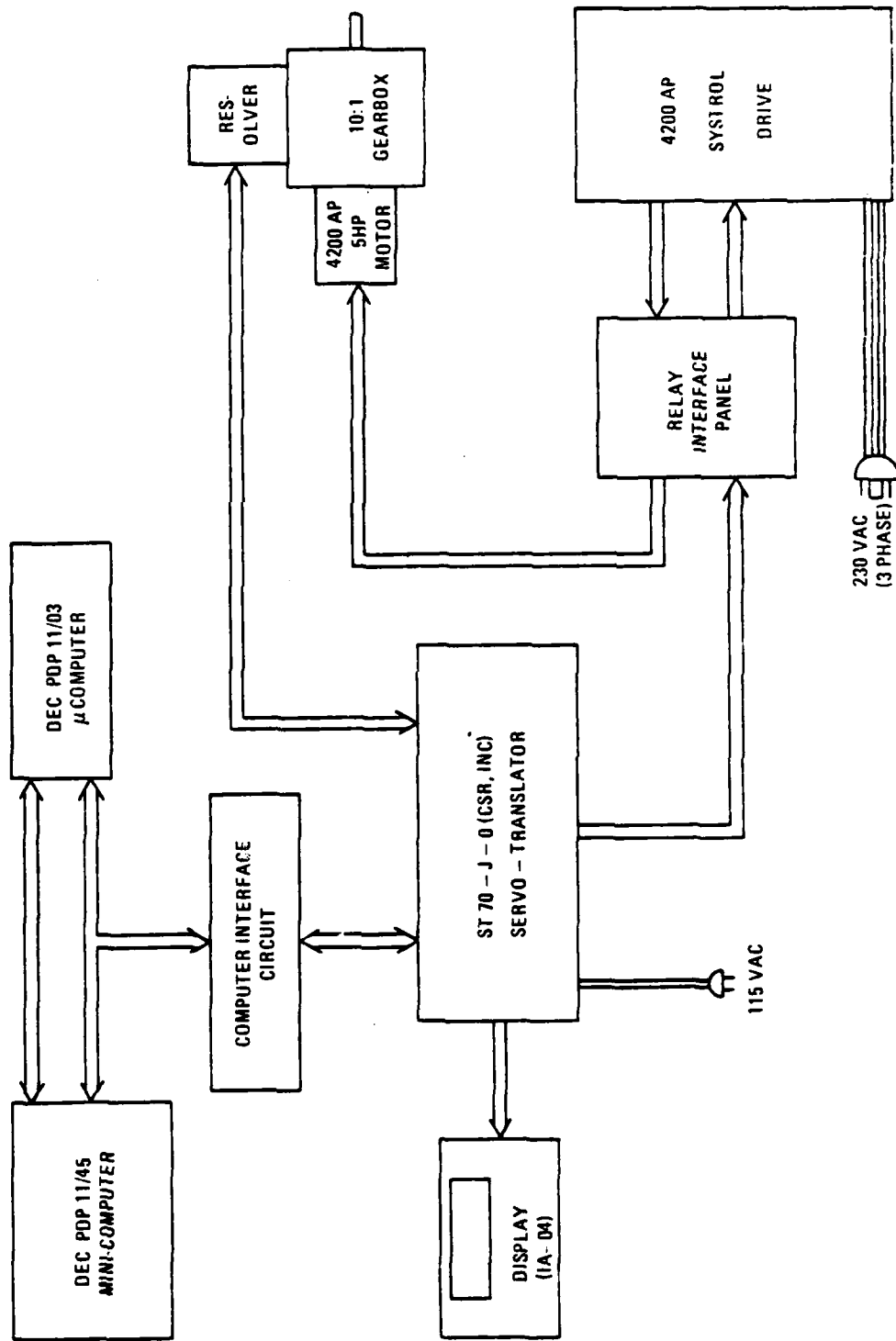


Figure 1/4. Translational Drive Control System - Functional Schematic

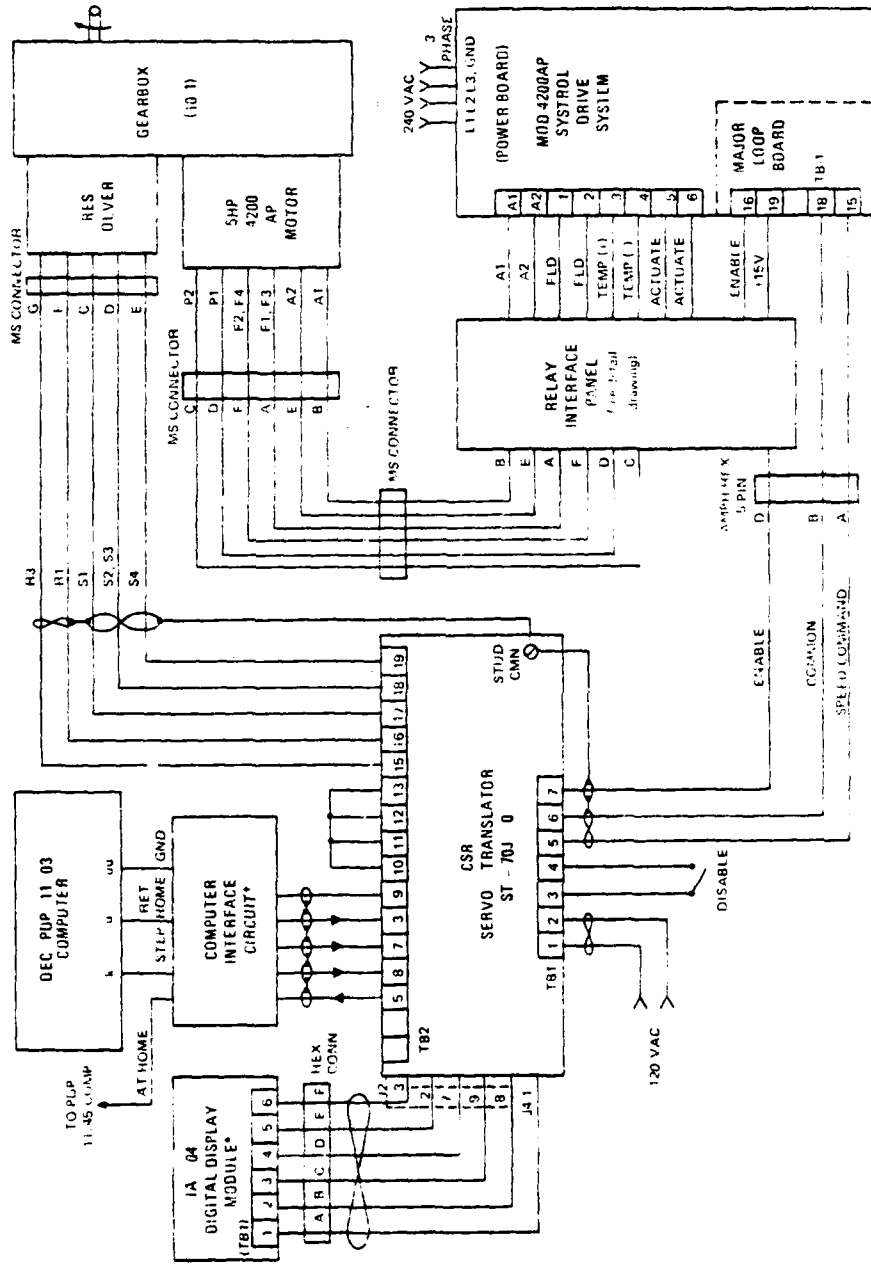


Figure 15. Translational Drive Control System - Interconnection Diagram

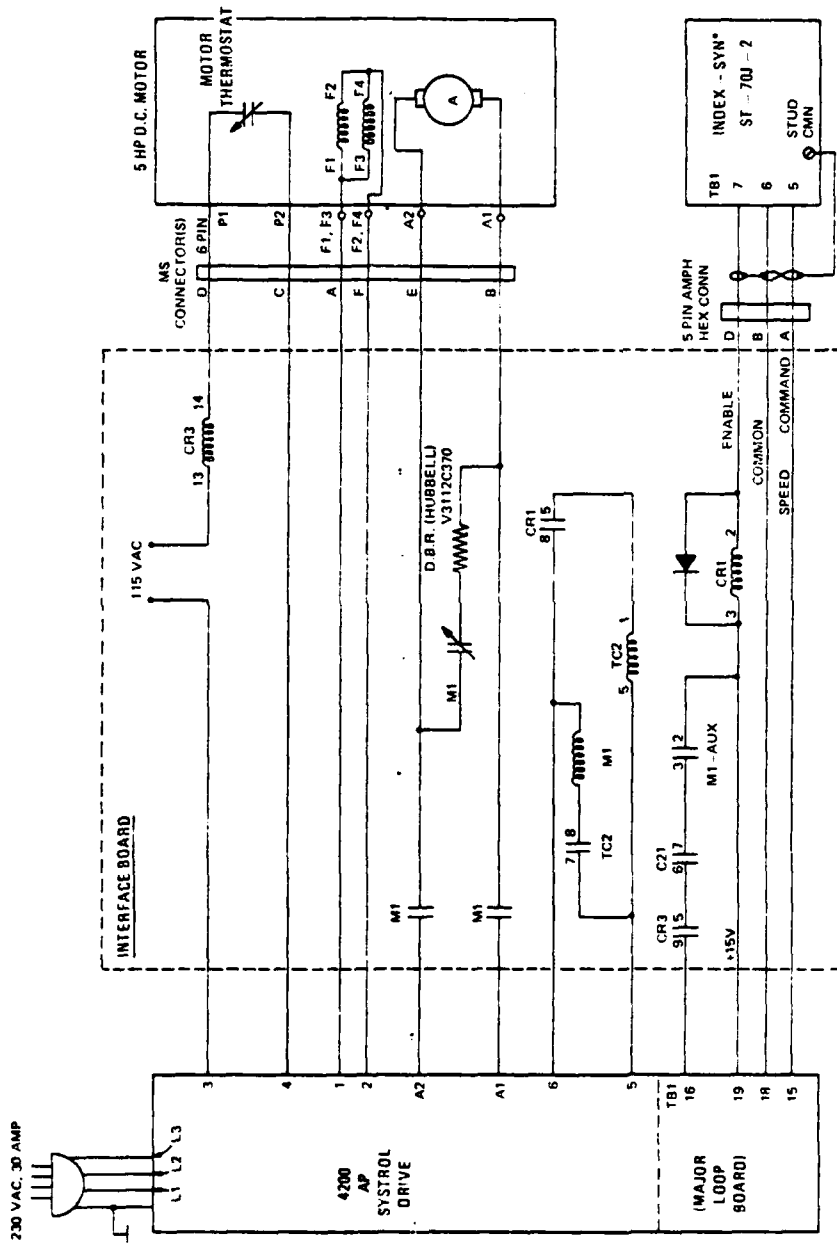
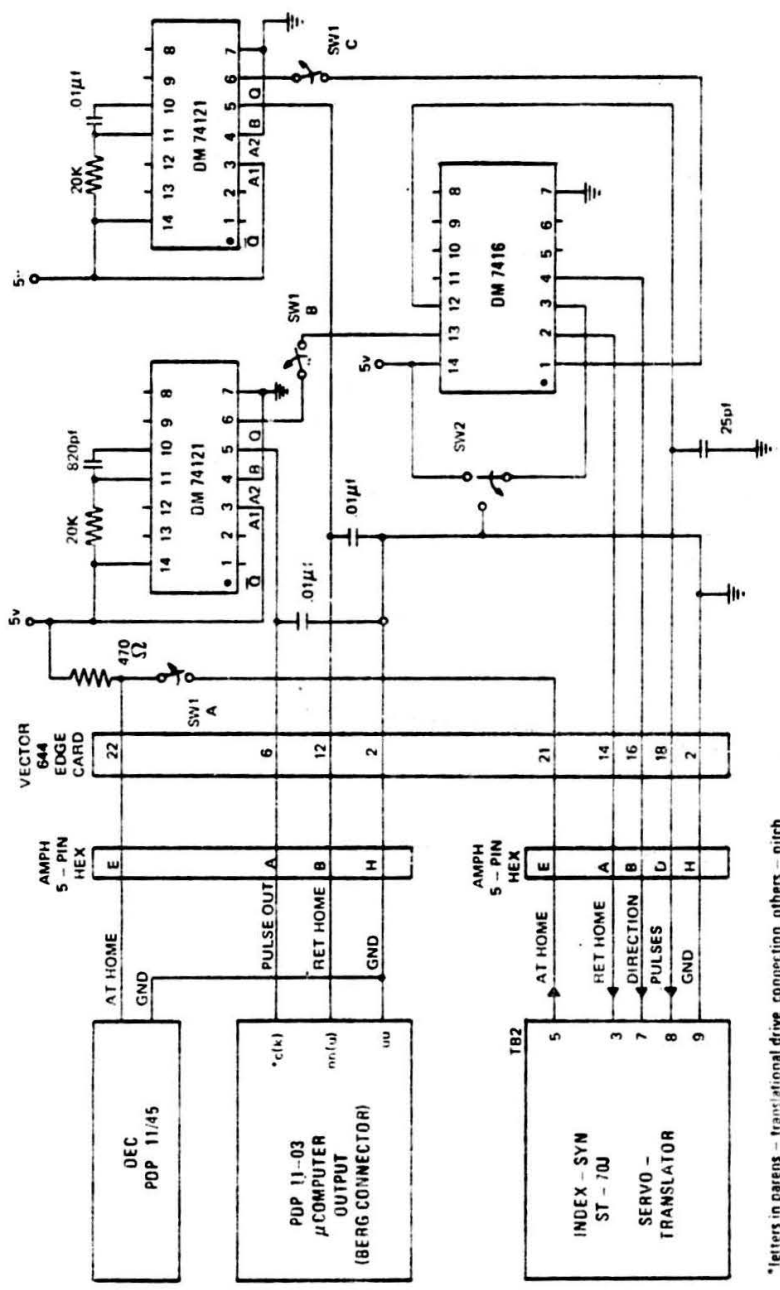


Figure 16. Relay Interface Circuit - Schematic



*letters in parens - translational drive connection, others - pitch

Figure 17. Microcomputer Interface circuit - Single Channel Schematic

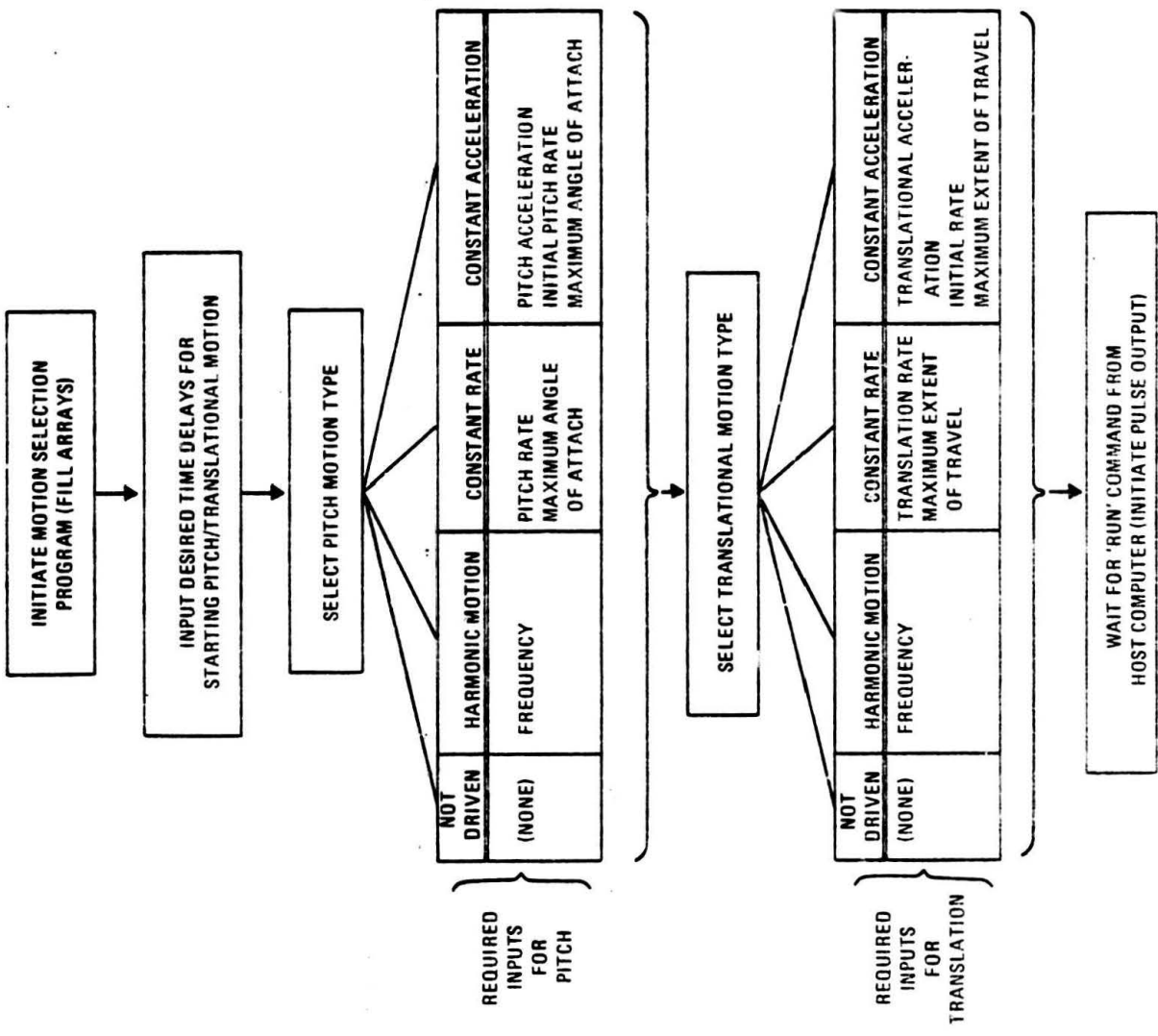


Figure 18. Selection of Motion Characteristics

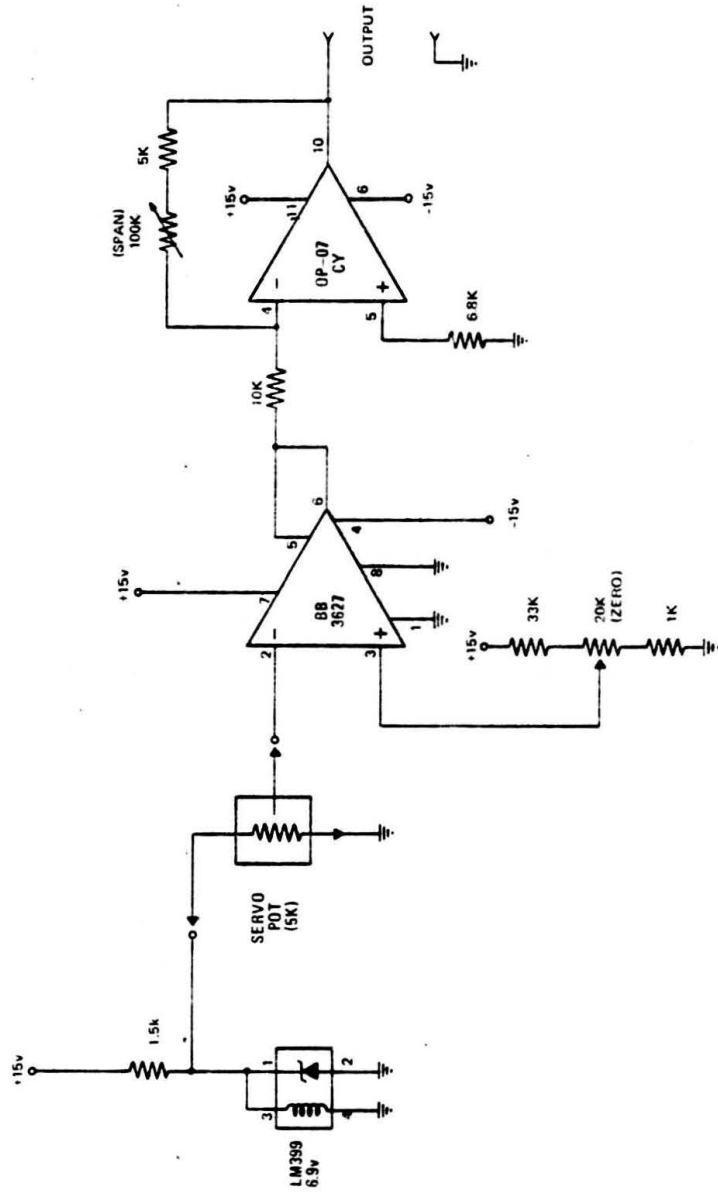


Figure 19. Position Potentiometer Amplifier Circuit

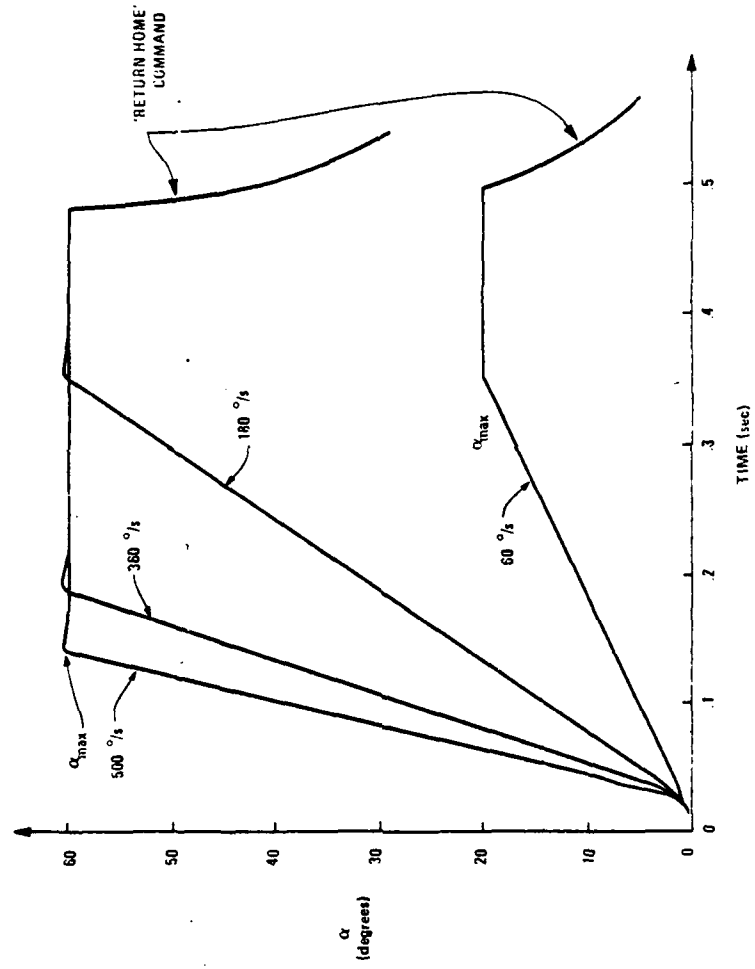


Figure 20. Pitch Oscillator Performance, Constant Rate Motion, Low to Moderate Frequencies.

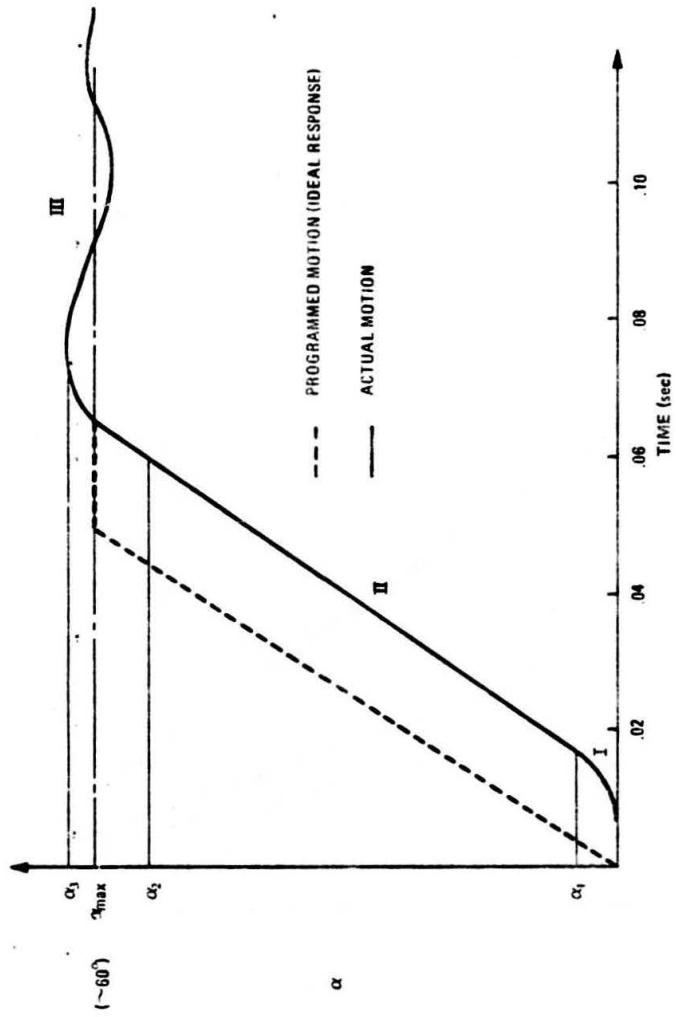


Figure 21. Pitch Oscillator Performance, Constant Rate Motion, High Frequency (Typical)

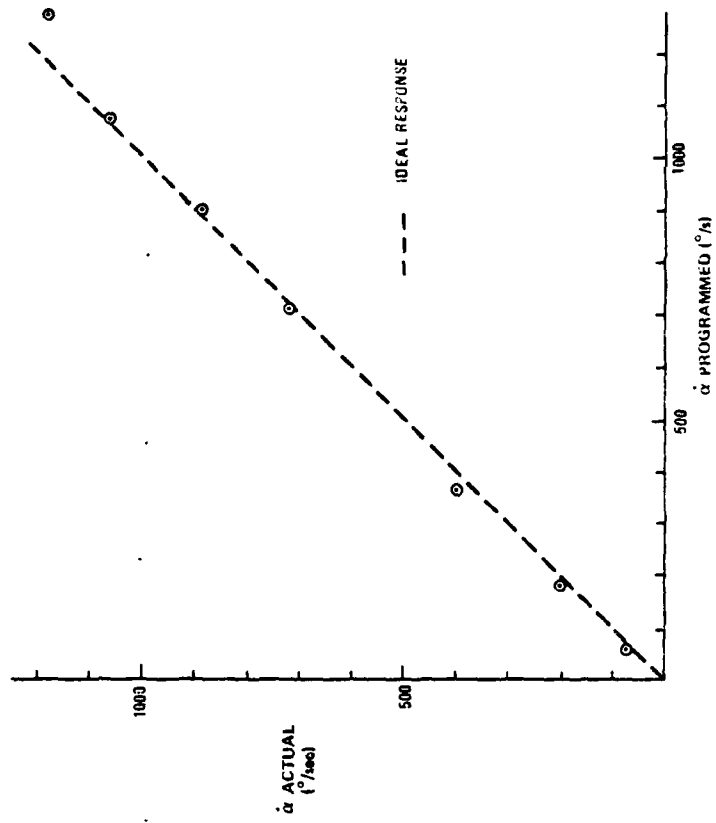


Figure 22. Pitch Performance Comparison, Constant Rate Motion

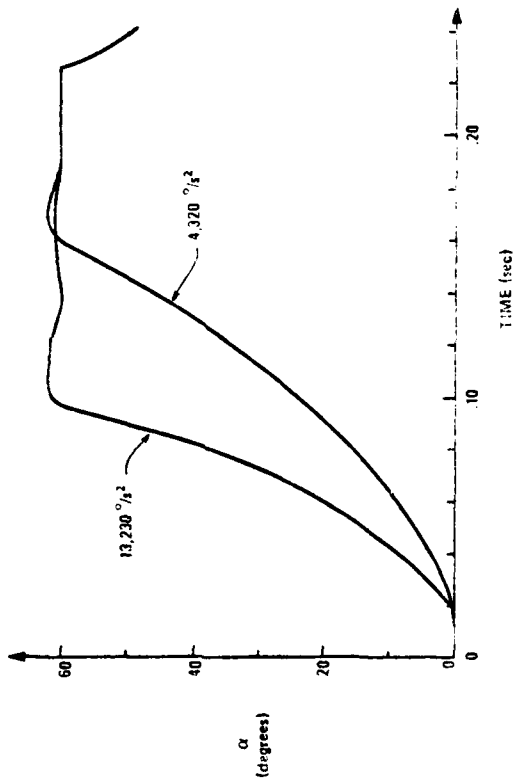


Figure 23. Pitch Oscillator Performance, Constant Acceleration

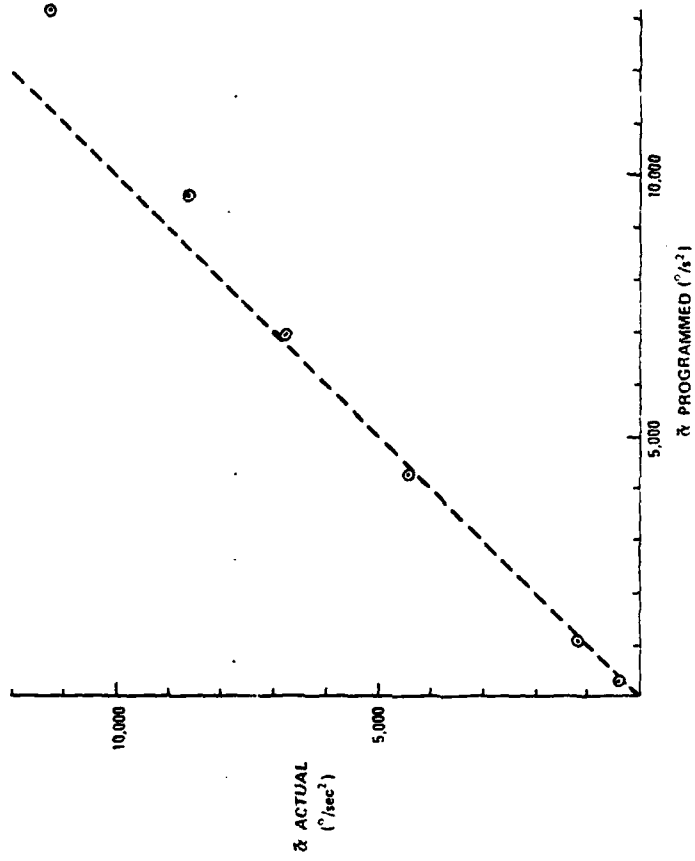


Figure 24. Pitch Performance Comparison, Constant Acceleration

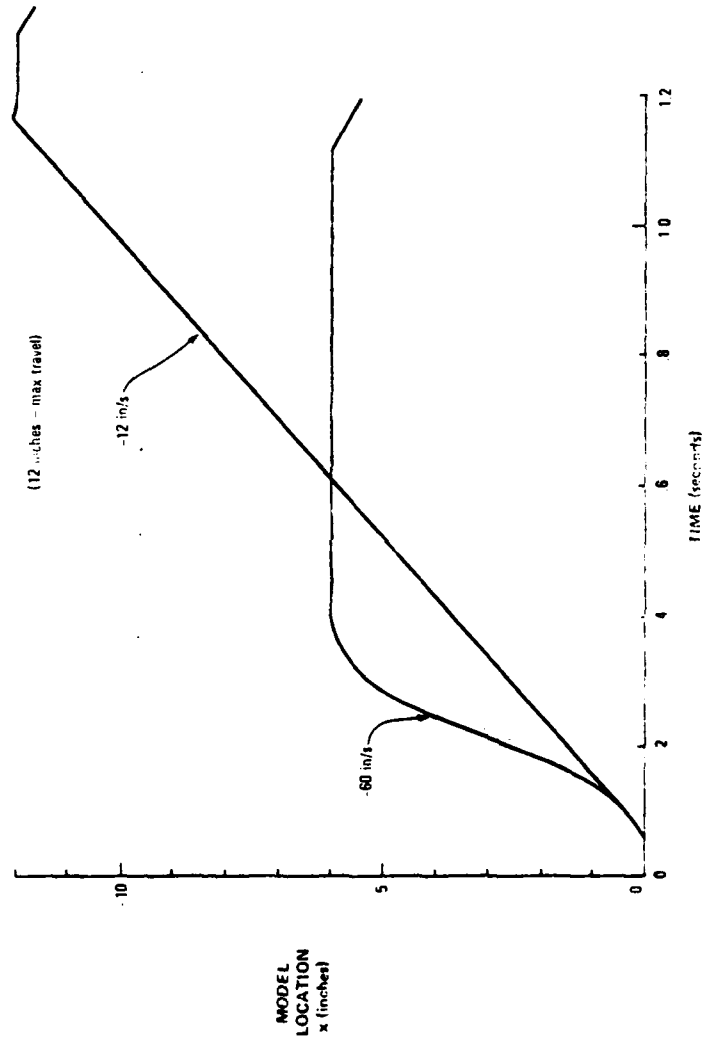


Figure 25. Translational Oscillator Performance, Constant Rate Motion

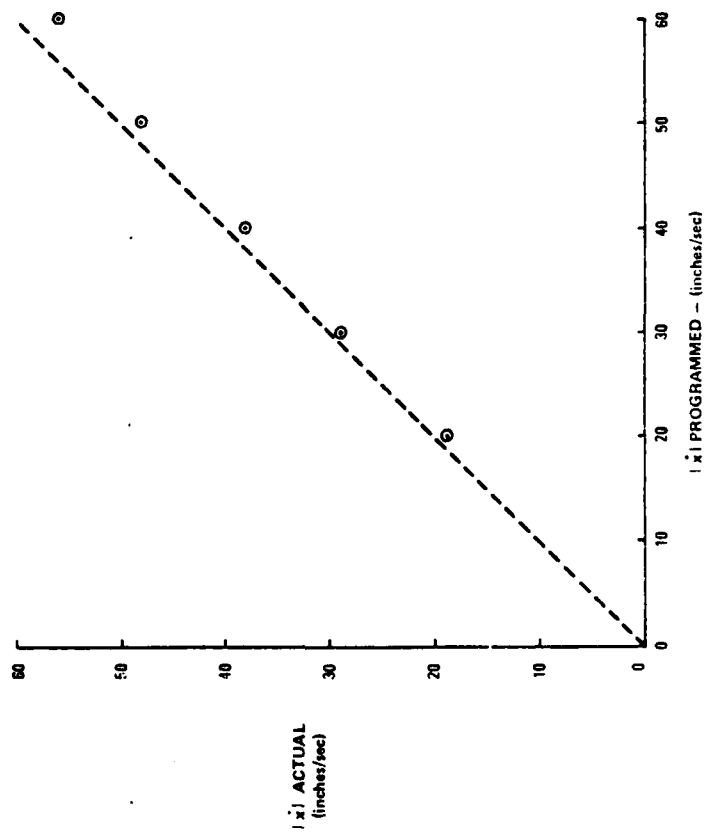


Figure 26. Translational Drive Performance - Tunnel Off, Constant Rate Motion

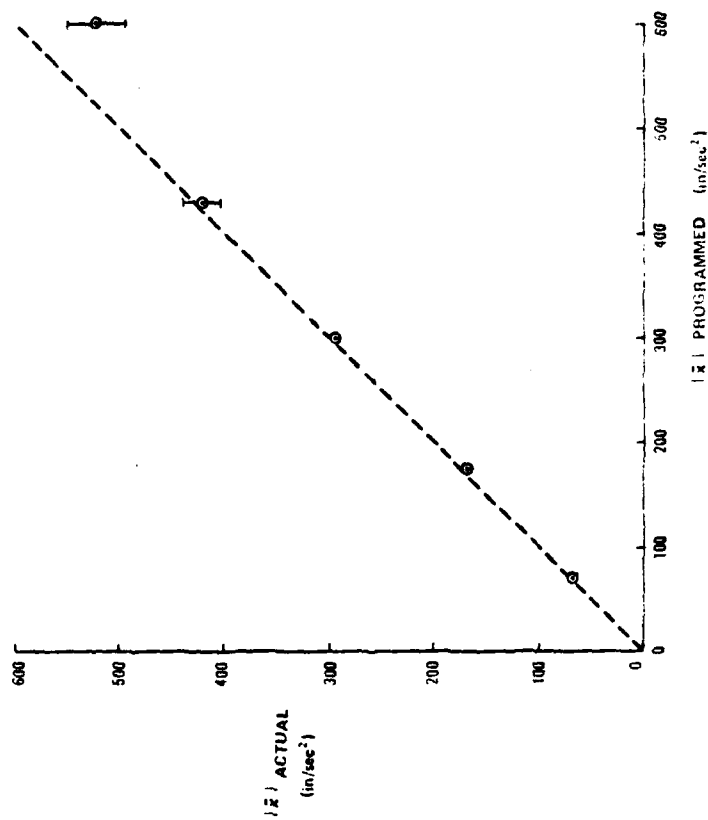


Figure 27. Translational Drive Performance - Tunnel Off, Constant Acceleration Motion

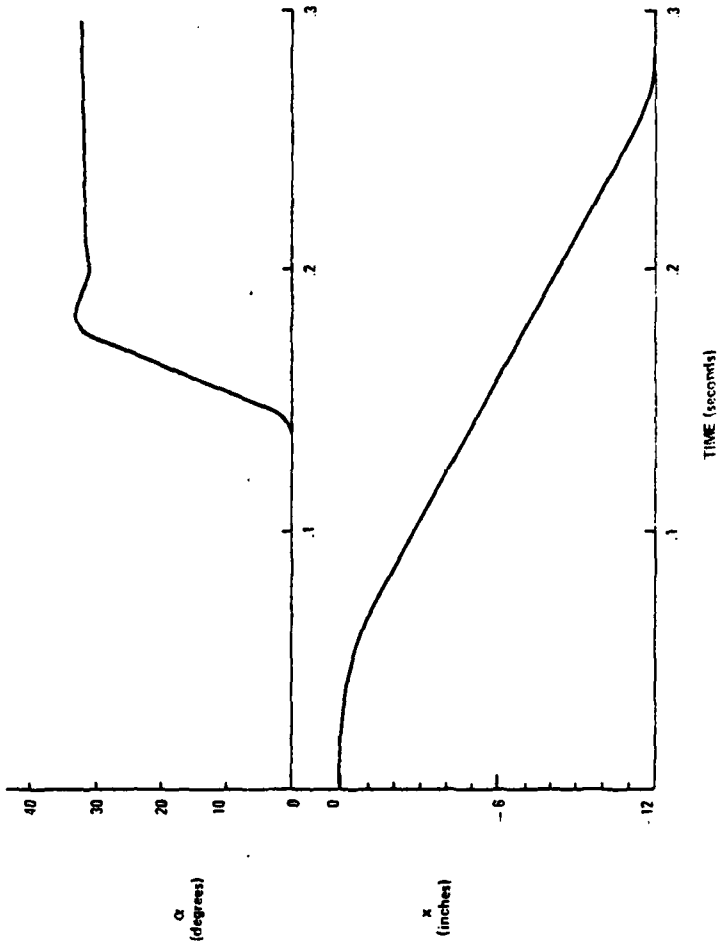


Figure 28. Combined Drive Performance - Illustration at High Frequency

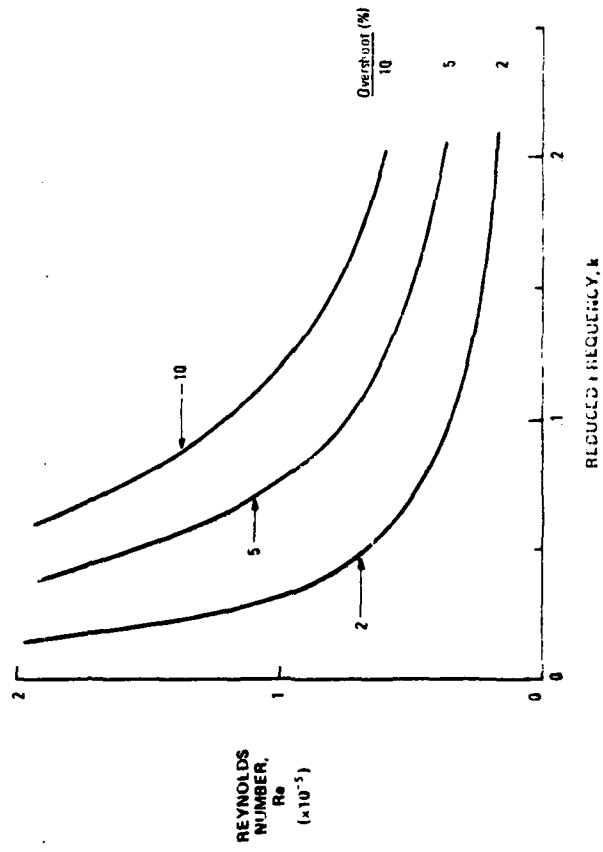


Figure 29. Pitch Axis Performance Map - Streaming Conditions